From the Medical University Graz

Division of Cardiology

Division Chief: Univ.-Prof. Dr. med. Burkert M. Pieske

REGULATION OF ANGIOGENESIS IN PRESSURE-OVERLOAD HYPERTROPHY

by

Dr. med. univ. Elisabeth A. Scherr

A Thesis Submitted to the

Medical University of Graz

Doctoral Program for Medical Sciences

GRAZ, 2009

DECLARATION

"I hereby declare that this submission is my own work and that, to the best of my knowledge, it does not contain any material written by another person nor material which to a substantial extent has been accepted for the award of any other degree or diploma of the university or other institute of higher learning, except where due acknowledgment that has been made in the text."

Graz, 12.12.2009

Dr. Elisabeth Scherr

SUPERVISOR

Univ.-Prof. Dr. med. Robert Gasser, PhD

THESIS COMMITTEE

Univ.-Prof. Dr. med. Robert Gasser, PhD

Univ.-Prof. Dr. med. Robert Zweiker

ABSTRACT

Objective: Inadequate capillary growth in pressure-overload left ventricular hypertrophy impairs myocardial perfusion and substrate delivery, contributing to progression and heart failure. New capillary development is tightly regulated by a variety of factors such as pro-angiogenic growth factors like Vascular Endothelial Growth Factor (VEGF) and endogenous angiogenesis inhibitors such as the splice variant of VEGF Receptor-1 (sVEGFR-1). Binding of VEGF to sVEGFR-1 restricts the amount of VEGF available for VEGFR-2 activation to induce angiogenesis. We sought to determine whether blocking of sVEGFR-1 with Placental Growth Factor (PlGF), which selectively targets sVEGFR-1, releases VEGF to induce angiogenesis and thereby delays heart failure.

Methods: Pressure-overload hypertrophy was achieved by banding the descending aorta in 10-day-old rabbits. At 4 wks and 6 wks of age, hypertrophied animals were treated with intra-pericardial administration of rhPlGF (2μg/kg). Shorting fraction (SF) determined by transthoracic echocardiography was used as a measure of contractile function. At 7 wks of age (de-compensation, heart failure), capillary density (immunohistochemistry) and VEGF release from sVEGFR-1 (ELISA) were measured in age-matched controls (C), untreated hypertrophied (H), and PlGF-treated hypertrophied hearts (PlGF). Data are expressed as mean±SEM with ANOVA for significance testing ($p \leq 0.05$).

Results: Contractile function was preserved in hypertrophied hearts treated with PlGF compared to untreated hypertrophy (PlGF: 43.4±2.1%SF versus H: 16.81±1.3%SF versus C: 42.4±1.9%SF; $p \leq 0.05$). Capillary density was significantly increased in PlGF treated versus untreated hypertrophied and control hearts (PlGF: 1.86±0.07 versus H: 0.733±0.02 versus C: 1±0.01 capillaries/nuclei; $p < 0.001$). PlGF treated hearts showed a significant increase in free, unbound VEGF protein compared to untreated hypertrophied hearts (PlGF: 0.021±0.001 versus H: 0.01±0.0005 pg/ml; $p \leq 0.05$).

Conclusion: These results indicate that treatment with PlGF releases sufficient VEGF from soluble VEGFR-1 to promote capillary growth and thereby preserves contractile function and delays the onset of failure in pressure-overload hypertrophy.

Keywords: angiogenesis, hypertrophy, growth factors

Presented at the Judah Folkman Research Day 2009, Boston, MA

ACKNOWLEDGEMENTS

Writing this thesis has been an educational and joyful experience for me. In this section I would like to acknowledge the people who have contributed to this thesis. It is my pleasure to express my gratitude to all those who have supported me.

This thesis would not have been possible without the excellent and constant support, guidance and encouragement of Univ.-Prof. Dr. Robert Gasser, PhD. I would like to take the opportunity and thank him very much for his outstanding support, advice and mentorship, which I am very indebted to. His scientific intuition has made him an important source of ideas, which have inspired me since I started my work in the laboratory.

Very special thanks go to Dr. Ingeborg Friehs. This study would not have been successful without her excellent knowledge, gracious support and assistance.

Further, I gratefully acknowledge Univ.-Prof. Dr. Zweiker for his support and advice.

I also would like to thank the Max Kade Foundation and its president Dr. Lya Friedrich-Pfeiffer for supporting this research project.

I very much would like to thank my parents Elisabeth and Eduard, and my brother Stefan, whose constant encouragement and support have helped me in every step of my studies at the University.

I cannot end without being deeply grateful to my husband A.K. Kaza for his love, advice and his enduring confidence. A.K. has given me unbelievable support while writing this thesis.

Finally, I would like to thank the many faculty and students who have inspired me to ask questions, think, solve problems, reason and learn.

Science may set limits to knowledge, but should not set limits to imagination.

Bertrand Russell (1872-1970)

I would like to dedicate this thesis to my loving parents.

CONTENTS

Chapter 3 METHODS 38

1. Left Ventricular (LV) Hypertrophy Animal Model
2. In-Vivo Myocardial Function Measurements by Serial Transthoracic Echocardiography
3. Myocardial Tissue Extraction
    a. *RNA Isolation*
    b. *Protein Isolation*
    c. *Nuclear Extraction*
4. Immunoblotting
5. VEGF Binding ELISA Immunoassay
6. Immunoprecipitation
7. Primer Design
8. Gradient PCR
9. Agarose Gel Electropzhoresis
10. Quantitative RT-PCR
11. RT-PCR – General Principles
12. Current Experiment – qRT-PCR
13. Melting (Dissociation) Curve
14. Blocking of sVEGFR-1 by Treatment with Placental Growth Factor (PlGF)
    a. *Principle and Timeline*
    b. *Determination of Capillary Density*

Introduction

INTRODUCTION

1. Preview

The overall goal of this project is to investigate the lack of angiogenic response in cardiac pressure-overload hypertrophy and to evaluate therapeutic strategies aimed at promoting angiogenesis in pressure-overload hypertrophied myocardium.

2. Pressure-Overload Hypertrophy

Pressure-overload hypertrophy is a major risk factor for cardiac morbidity and mortality. It is an adaptive response, which compensates for increased workload. In response to persistent elevation in wall stress, the heart attempts to compensate by remodeling, decreasing wall stress and preserving contractile function (Arnett, 2004).

Changes occur in ventricular chamber dimensions and composition of the myocardium affecting extracellular matrix, cardiomyocytes and microvasculature. During the initial phase of this dynamic process, the ventricle attempts to compensate for the increased workload by an increase in mass-to-volume ratio and thus maintaining adequate contractile function and normal geometric shape.

If pressure-overload remains, de-compensation follows with ventricular dilation and contractile dysfunction. In response to mechanical stress, cardiomyocytes progressively enlarge in size as hypertrophy develops (Friehs, 2006).

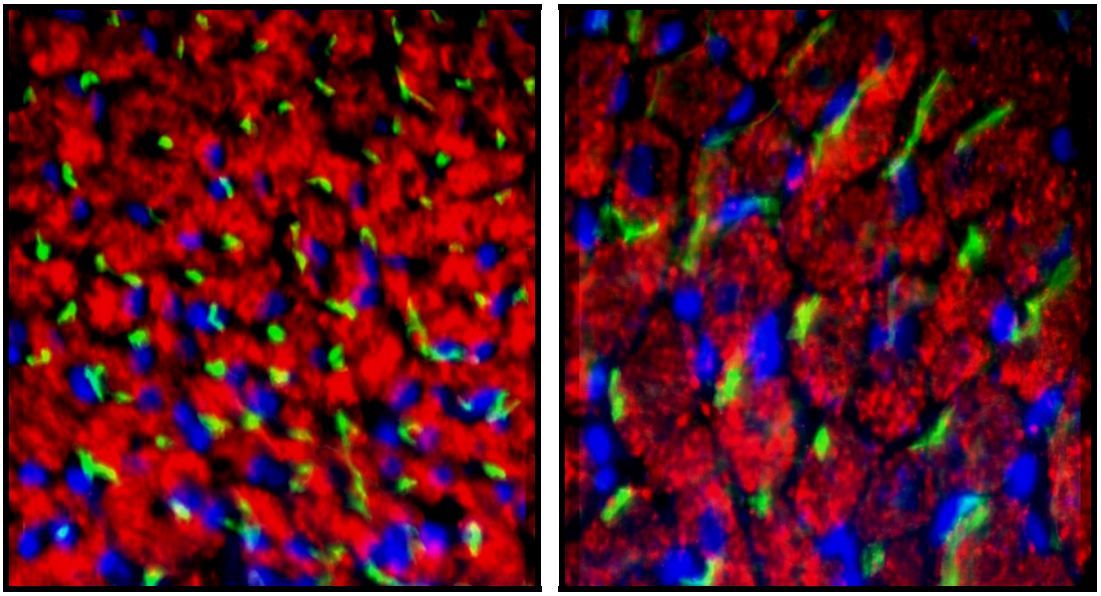

Figure 1. Immunohistochemistry (IHC) slides of control (left) and hypertrophied (right) left ventricular myocardium are depicted in this figure. Cardiomyocytes are stained with Desmin (red), nuclei with DAPI (blue) and capillaries with CD31 (green)

As hypertrophy progresses, however, there is no concomitant increase in capillaries. The volume of tissue supplied by each capillary increases (Friehs, 1999). This results in impaired supply of nutrients and oxygen particularly during increased workload. The ability of endothelial and non-myocyte cells to respond to exogenous angiogenesis inducing growth factors such as Vascular Endothelial Growth Factor (VEGF) is preserved (Friehs, 1999).

3. Angiogenesis and its Regulation

Angiogenesis is a physiological process, which is defined as a growth of endothelial sprouts from preexisting capillaries (Dvorak, 2005). Physiological stimuli of angiogenesis are hypoxia, ischemia and inflammation.

On the contrary, vasculogenesis is a term which is used for de novo formation of vascular structures from circulating angioblasts (mesenchymal endothelial precursor cells), which differentiate into endothelial cells and build a primitive vascular network. This occurs particularly during embryonic vascular development (Karamysheva, 2008). All larger vascular structures of the embryo including the dorsal aorta, cardinal veins and the endocardium of the heart arise by this process (Fruttiger, 2001). The Vascular Endothelial Growth Factor (VEGF) regulates angioblast differentiation. Angioblasts have been shown to express VEGFR-2, which is the main receptor involved in angiogenesis.

Vascular growth is tightly regulated by a variety of factors such as pro-angiogenic factors like Vascular Endothelial Growth Factor (VEGF), Fibroblast Growth Factor (FGF), Platelet-derived Growth Factor (PDGF) and anti-angiogenic factors such as the soluble VEGFR-1, Angiostatin or Endostatin (Karamysheva, 2008).

Table 1 gives a few examples of pro- and anti-angiogenic factors. These endogenous pro- and anti-angiogenic factors hold a delicate balance for an adequate supply of nutrients and oxygen for all mammalian cells and tissue. Angiogenesis is involved in physiological (embryonic development, menstruation,

pregnancy, wound healing) and pathological (cancer, blindness) processes (Dvorak, 2005).

Angiogenesis Inhibitors	Angiogenesis Activators
Angiostatin	Fibroblast Growth Factor (FGF)
Endostatin	Vascular Endothelial Growth Factor (VEGF)
Tumstatin	Platelet-derived Growth Factor (PDGF)
Soluble VEGFR-1 (sVEGFR-1)	Epidermal Growth Factor (EGF)
Angiopoietin 2	Transforming Growth Factor beta (TGF-β)
Platelet factor 4	Nitrous Oxide Systems (NOS)
Interferons	Angiopoietin (Ang 1)

Table 1. Examples of pro- and anti-angiogenic factors, which influence vascular growth

In healthy tissues, the balance shifts towards the anti-angiogenic side. Tumor cells, however, are able to cause a shift towards pro-angiogenesis.

Several groups have shown that angiogenesis occurs in several steps (Folkman et Haudenschild, 1980 as well as Folkman et Shing, 1992). Proteolytic degeneration of the basement membrane is followed by migration of endothelial cells (EC), proliferation of migrated endothelial cells and formation of new tubes. New capillaries are surrounded by pericytes (differentiation), which indicates the last step in development of new vessels.

4. Vascular Endothelial Growth Factor (VEGF) and VEGF Isoforms

The Vascular Endothelial Growth Factor (VEGF) is a key regulator of angiogenesis in the myocardium (Ferrara, 2003). Independent research laboratories contributed to the discovery of VEGF (Senger, 1986 and 1990; Ferrara, 1989).

In 1989, VEGF was first isolated from a medium conditioned by bovine pituitary follicular cells and reported as a diffusible endothelial mitogen (Ferrara and Henzel, 1989). VEGF is a disulfide-bonded glycoprotein of 34-54 kDa.

The VEGF gene is located on the short arm of chromosome six (Vincenti, 1996) and is composed of eight exons and seven introns (Tischer, 1991).

VEGF-A belongs to the VEGF gene family which includes VEGF-A, VEGF-B, VEGF-C, VEGF-D, and Placenta Growth Factor (PlGF). VEGF-C and VEGF-D are known to regulate lymphangiogenesis (Meyer, 1999).

VEGF promotes growth of vascular endothelial cells and induces angiogenesis (Ferrara et Henzel, 1989). It is also known to be a survival factor for endothelial cells.

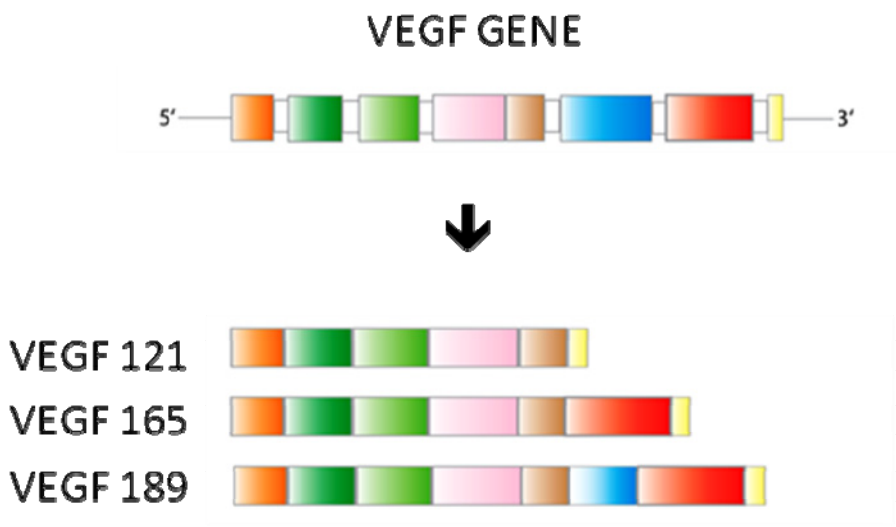

Figure 2. Vascular endothelial growth factor (VEGF) gene and VEGF isoforms 121, 165, 189 (modified after http://www.rosenthallab.com/)

As mentioned before, the vascular endothelial growth actor (VEGF) is the most important inducer of angiogenesis in the heart. This growth factor is released by all major cell types in the myocardium, including endothelial cells, cardiomyocytes and fibroblasts. It stimulates endothelial cell migration, proliferation, tube formation and protects endothelial cells from apoptosis.

Several VEGF isoforms are generated through alternative splicing of mRNA, from the VEGF gene. $VEGF_{121}$, $VEGF_{165}$ and $VEGF_{189}$ are isoforms present in the heart (Marti, 2002). $VEGF_{121}$ and $VEGF_{165}$ are the most abundant and potent isoforms with $VEGF_{165}$ having the highest receptor affinity (Bacic, 1995).

VEGF can be available in the heart as a free soluble protein such as VEGF121 and parts of $VEGF_{165}$. Only free soluble VEGF protein is active and able to induce angiogenesis. A significant amount of VEGF remains bound to the extracellular matrix (parts of $VEGF_{165}$and $VEGF_{189}$) and is inactive. Bioactive $VEGF_{189}$ is generated by proteolytic cleavage (Park, 1994). Therefore, VEGF protein becomes available to endothelial cells by two distinct mechanisms: as a freely soluble protein or following protease activation by release from extracellular membrane bound stores.

5. VEGF Receptors and Signaling

VEGF exerts its cellular effects by binding to two known transmembrane tyrosine kinase receptors: VEGFR-1 and VEGFR-2 (Folkman, 1992; Fong, 1995, Kendall, 2006).

Both receptors, VEGFR-1 and VEGFR-2, are structurally similar. The VEGF Receptors consist of an extracellular immunogloblin (Ig) like domain (the VEGF binding site), a single transmembrane region and an intracellular region, which represents the tyrosine kinase domain.

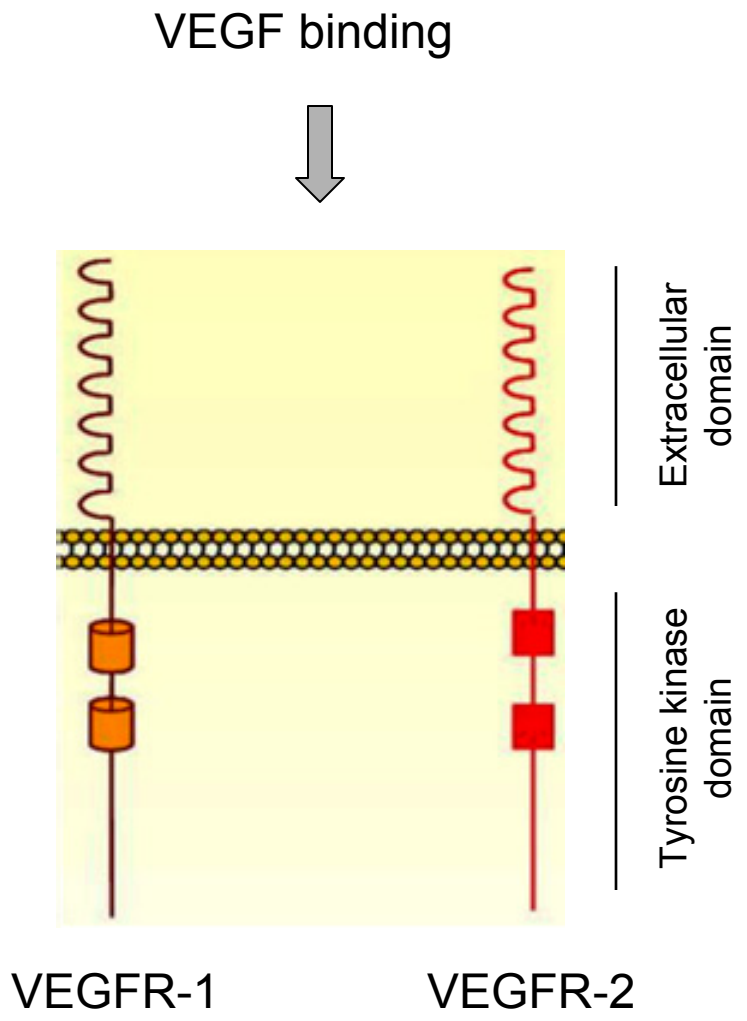

Figure 3. VEGF receptors 1 and 2. Binding of VEGF to its receptors occurs at the extracellular Ig-like domain

VEGFR-1 and VEGFR-2 are required for normal development and angiogenesis. VEGFR-2 is the main receptor involved in VEGF-stimulated angiogensis and stimulates endothelial cell proliferation, differentiation, migration and tubulogenesis. (Ferrara 2003, Shinkaruk 2003).

VEGF binds to the extracellular domain of VEGFR-2. This step is followed by dimerization of the receptors and phosphorylation of the tyrosine kinases, which ultimately leads to activation of various downstream pathways.

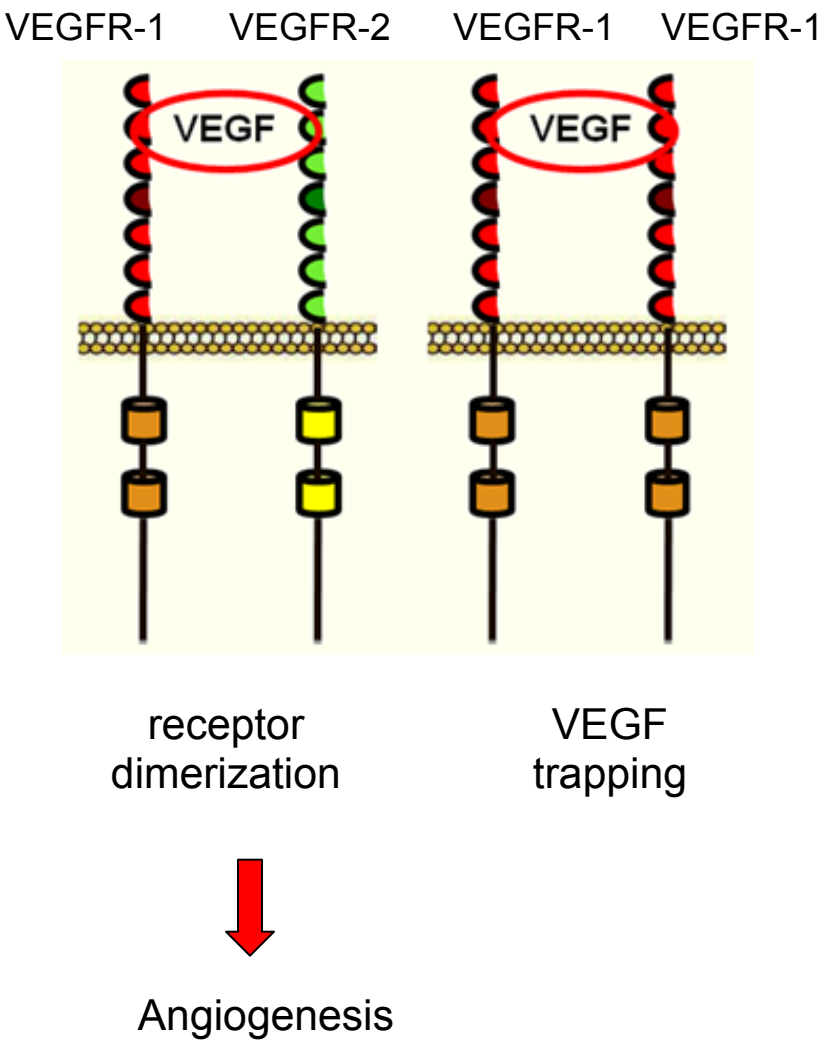

Figure 4. VEGF binding to VEGFR-1 and VEGFR-2

a. Vascular Endothelial Growth Factor Receptor 1 (VEGFR-1)

VEGFR-1 was identified earlier then VEGFR-2, however, the precise role remains still unknown. Gene-targeting studies have demonstrated the important role of VEGFR-1 during embryogenesis.

VEGFR-1 null mutant mice die at embryonic stage due to an overgrowth and disorganization of blood vessels and not due to poor vascularization (Friehs, 2003). These results indicate VEGFR-1 to be a negative regulator of VEGF action during early development.

VEGFR-1 is known to be a 180-kDa transmembrane protein that is composed of seven extracellular Ig-like domains, which include the binding site for VEGF in the second Ig-like domain, a single transmembrane domain and an intracellular tyrosine kinase region (Park, 1993; Shinkaruk, 2003). The affinity of VEGFR-1 for VEGF is very high, with a Kd of about 2-10 pM, which is at least one order of magnitude higher than that of VEGFR-2 (De Vries, 1992). The tyrosine kinase activity of VEGFR-1, however, is relatively weak, and VEGF does not stimulate the proliferation of cells over-expressing VEGFR-1 (Rakusan, 1992; Waltenberger, 1994).

Interestingly, VEGFR-1 lacking the tyrosine kinase domain but not the VEGF binding extracellular domain does not result in lethality or any other defect in vascular development. These findings suggest that VEGFR-1 has a dual function in angiogenesis, acting in a positive and negative manner. Since VEGFR-1 and VEGFR-2 can form heterodimers, VEGFR-1 may participate in the regulation of

the proliferative response of endothelium to VEGF. VEGFR-1 is also able to form homodimers (no cross-talk with VEGFR-2). This does not lead to cell migration, cell proliferation and intercellular calcium release (trapping) and is thereby a negative regulator.

b. Soluble VEGFR-1 (sVEGFR-1)

Another important feature of VEGFR-1 is that the gene not only encodes the mRNA for a full-length receptor but also for a short alternatively spliced soluble form of the VEGFR-1 protein which is called the soluble VEGFR-1 (sVEGFR-1).

This soluble form carries only the extracellular domain (Rakusan, 1992; Waltenberger, 1994) and lacks the transmembranous domain as well as the intracellular tyrosine kinase region. In addition, it has a unique 31 amino-acid C-terminus (Rakusan, 1992; Waltenberger, 1994).

It was first reported in patients with pre-eclampsia who showed abnormally high levels of sVEGFR-1 associated with inadequate vascularization of the placenta (Maynard, 2003 and 2005).

It is thought that the soluble VEGFR-1 is most likely a negative regulator of VEGF bioavailability because it is able to form heterodimers with membrane-bound VEGFR-1 and VEGFR-2. It acts as a receptor blocker of both VEGFR-1 and VEGFR-2. It also sequesters VEGF (trapping) and limits the amount of free, soluble VEGF for induction of angiogenesis.

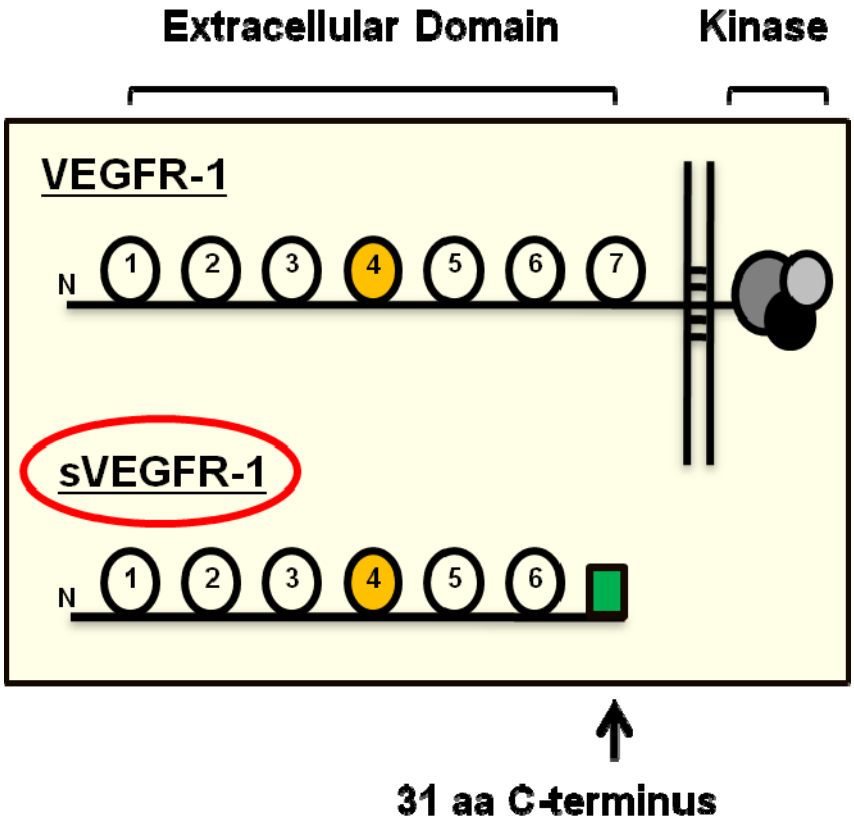

Figure 5. VEGFR-1 and its alternatively spliced soluble form (sVEGFR-1). The soluble form carries only the extracellular domain and an unique 31 amino-acid C-terminus. However, it lacks the transmembranous domain as well as the intracellular tyrosine kinase region of VEGFR-1

c. VEGF Receptor 2 (VEGFR-2)

VEGFR-2 is thought to be the main mediator of angiogenesis in the myocardium. VEGFR-2 knock-out mice have been shown to die in utero because of lack of vasculogenesis and failure to develop new blood islands and organized blood vessels. It binds VEGF with a lower affinity than VEGFR-1, however with a strong

ligand-dependent tyrosine autophosphorylation. The VEGF binding site has been mapped to the second and third immunglobulin domain.

6. Placental Growth Factor (PlGF)

a. Physiological Characteristics of PlGF

The placental growth factor (PlGF) is a dimeric protein which belongs to the VEGF family (Ribatti, 2008). It is an angiogenic protein which was originally discovered in the placenta, cloned and purified in 1991 by Maria Graziella Persico (Maglione D 1991, Ribatti, 2008). The structure of PlGF exhibits remarkable similarities to VEGF (Maglione, 1993).

The human PlGF gene is located on chromosome 14 and carries seven exons (Maglione, 1993; Ribatti, 2008).

In the placenta, PlGF was thought to control trophoblast growth and differentiation (Maglione, 1993). PlGF is expressed in villous trophoblast cells whereas VEGF is located within the chorionic plate in cells mesenchymal origin (Vuorela, 1997).

In addition to the placenta, PlGF is expressed in several other tissues such as the heart, lung, skeletal muscle or the adipose tissue (Persico, 1999 and Voros, 2005).

b. Mechanism and Role of PlGF in the Interaction with VEGFR-1

VEGF has been shown to interact with both tyrosine kinase receptors, VEGFR-1 and VEGFR-2. PlGF, however, only binds to VEGFR-1, not to the main receptor involved in angiogenesis, VEGFR-2 (Tjwa, 2003; Autiero, 2003).

Under conditions, where VEGF levels are increased (ischemia and/or tumor conditions), PlGF knockout mice show significantly impaired arteriogenesis as well as angiogenesis.

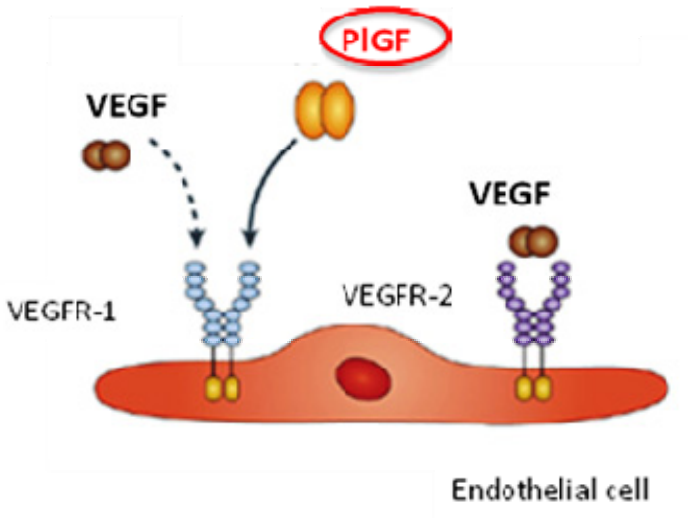

Figure 6. Binding of placental growth factor to VEGFR-1, but not to VEGFR-2

However, loss of PlGF under normal conditions, does not affect development, reproduction or postnatal life (Ribatti, 2008).

7. VEGF and hypoxia

Hypoxia is a potent inducer and regulator of VEGF expression. Hypoxic transcriptional regulation of VEGF is mediated by the heterodimeric transcription factor hypoxia-inducible factor 1 (HIF-1) (Maxwell, 2001).

HIF-1 consists of two subunits: HIF-1 alpha (HIF-1α) and HIF-1 beta (HIF-1β). While HIF-1β is expressed constitutively in the nucleus, HIF-1α expression is directly regulated by tissue oxygen.

Under normoxic conditions, HIF-1α is degraded rapidly by the ubiquitin pathway. Under hypoxic conditions, however, HIF-1α stabilizes, translocates to the nucleus and forms heterodimers with HIF-1β. This is followed by activation of VEGF gene transcription.

8. The glucose transport molecules GLUT1 and GLUT4 in pressure – overload left ventricular myocardium

A second very important topic in this thesis is the regulation of glucose in the left ventricular hypertrophied myocardium.

Glucose is an important source of energy for the heart. Glucose utilization and transport by cardiomyocytes is critical for normal cardiac function. However, fatty acid oxidation is the primary source of acetyl CoA for the tricarboxylic acid cycle (TCA cycle) in the normal working heart.

The plasma membrane is impermeable to polar molecules such as glucose. The cellular uptake or facilitated diffusion of glucose across the plasma membrane is mediated by a family of transport proteins, which have affinity for glucose. These glucose transporters, which are characterized to have distinct tissues distribution, reside in and span the plasma membrane.

In addition, they are rate limiting of glucose entry in the cell. Trans-sarcolemmal glucose transport in cardiomyocytes is mediated by GLUT1 and GLUT4, which are expressed in high levels in the cardiac tissue.

Basal glucose transport is mediated primarily by GLUT1, which is constitutively present in sarcolemma but not in transverse tubules. GLUT4, which is the insulin-dependent trans-membrane glucose facilitative transport molecule, plays an important role in insulin–dependent cardiac glucose metabolism. Under basal conditions, only a small amount of GLUT4 is located in the sarcolemma. GLUT4 is primarily localized in small tubulo-vesicular elements adjacent to the

sarcolemma and transverse tubules, and in the trans-Golgi system. The translocation of glucose transporters, in particular GLUT4, to the sarcolemma and T-tubules is mainly regulated by insulin, exercise and ischemia.

Myocardial left ventricular hypertrophy remains a significant risk factor for congenital cardiac surgery. Hypertrophied myocardium exhibits a worse recovery of contractile function post-ischemia. Glucose entry into the myocardium is impaired in hypertrophied myocardium and this impairment occurs at the point of severe hypertrophy and the onset of ventricular dilatation (uncompensated hypertrophy).

We have developed an animal model of left ventricular hypertrophy in New Zealand White (NZW) rabbits. Pressure-overload hypertrophy was achieved by banding the thoracic aorta at seven to ten days of age. The band was placed loosely around the descending aorta. Progressive hypertrophy of the left ventricle begins at age 2-3 weeks and peak hypertrophy is seen at 4-5 weeks of age (plateau). After this compensated phase, severe hypertrophy with dilatation occurs by 6 weeks of age. This model mimics the clinical progression of hypertrophy in children with obstructive types of congenital heart disease.

Serial trans-thoracic echocardiography was performed weekly, starting at 3 weeks of age, to monitor left ventricular dimension, wall thickness, and LV cavity volume during the cardiac cycle. Two-dimensional cross-sectional images and M-mode of the left ventricle are obtained by echocardiography.

Effects of anesthesia or sedatives were avoided by conditioning the animals through daily handling and manipulation with a mock echo probe. Measurements of LV mass to LV volume ratio were used as an index for progression of hypertrophy. By four weeks of age, the increase in muscle mass is able to compensate to reduce wall stress (compensate state).

By six weeks of age, the increase in ventricular muscle mass is no longer able to compensate to reduce wall stress which leads to progressive LV dilatation. Myocardial contractile function was indexed as the shortening fraction to end-systolic stress relationship over time. Dysfunction develops by a significant decline in shortening fraction by six weeks of age (de-compensated state).

Cardiac tissue (LV hypertrophy and control) was harvested for RNA isolation at 6 weeks of age (n=5/group). Following progression of hypertrophy by trans-thoracic echocardiography, we determined that by 6 weeks of age, hypertrophied hearts showed signs of ventricular dilatation and contractile dysfunction. However, clinical signs have not developed yet. Total RNA was isolated using TRIzol (Invitrogen, CA). 100ng/rxn of RNA was transcribed and a One-Step PCR for GLUT1 and GLUT4 was performed using a SYBR Green qRT-PCR Kit (Quanta, MD).

Prior to qRT-PCR, specific primers for GLUT1 and GLUT4 were designed and tested. FASTA sequences for GLUT1 and GLUT4 (NM001105687 for GLUT1, NM001089313 for GLUT4) were entered into ensemble and an alignment with

rabbit was performed. This transcript sequence was then blasted with the original sequence, which resulted in a 99% identity.

Primer sequences were obtained from Operon. Conditions for quantitative PCR reaction were the following: incubation at 48ºC for one hour, then 94ºC for ten minutes. This step was followed by 40 cycles of 94ºC for 15 seconds, 53.4ºC for 30 seconds (annealing temperature) and 72º for 45 seconds using Stratgene Mx3000P RT-PCR machine. Data were analyzed using the delta-delta CT method according to Pfaffel and shown in % of control.

Specific primers were designed for qRT-PCR. Primer pairs for GLUT1 and GLUT4 are depicted below:

GLUT4 – Product Size: 66

AGCAGCTCTCAGGCATCAAT

CTACCCCTGCTGTCTCGAAG

GLUT1 – Product Size: 174

GCCCTGGATGTCCTATCTGA

CCCACAATGAAATTCGAGGT

Hypothesis

HYPOTHESIS

1) Up-regulation of VEGFR-1 and its alternatively spliced soluble form (sVEGFR-1) prevent capillary growth in pressure-overload left ventricular hypertrophied myocardium.

2) Treatment with the placental growth factor (PlGF) preserves contractile function, promotes capillary growth and delays the onset of heart failure in pressure-overload left ventricular (LV) hypertrophy.

3) Further, we hypothesized that the glucose transporter GLUT1 and GLUT4 are affected in hypertrophied LV myocardium at the time-point of severe hypertrophy with dilatation (uncompensated hypertrophy). Thus, to develop new treatment strategies for maintaining normal glucose uptake in pressure-overload hypertrophy, it appears to be very critical to further understand the mechanism by which the impaired glucose uptake occurs in uncompensated hypertrophy.

Methods

METHODS

1. Left Ventricular (LV) Hypertrophy Animal Model

Our group has developed a model of left ventricular (LV) hypertrophy in neonatal New Zealand White rabbits. Pressure-overload hypertrophy was achieved by banding the descending thoracic aorta at ten days of age.

Progressive LV hypertrophy starts at 3 weeks of age, and severe hypertrophy with ventricular dilation occurs at 7-8 weeks of age. This model mimics the clinical progression of hypertrophy in children with obstructive type of congenital heart disease.

Induction of general anesthesia was performed with ketamine (40-60 mg/kg) and xylazine (2-5 mg/kg) IM and maintained by isoflurane 0.25-2% via facemask. After anesthesia was induced, the chest was shaved and disinfected with betadine. In order to get access to the descending aorta, a left posterior thoracotomy in the 4^{th}intercostal space was performed. After dissecting the aorta free form the chest wall, we placed a loose 2-0 silk ligature not constricting the vessel around the aorta just distal to the ligamentum arteriosum.

Attention was paid that the band was not tied too tight around the vessel and did not cause any stenosis of the descending aorta. After the chest wall was closed, air from the chest cavity was evacuated from the left thoracic cavity by aspiration with a catheter connected to a syringe.

Post-treatment analgesia was administered (Buprenorphine 0.01-0.05 mg/kg IM) immediately after the procedure. Animals were placed in an incubator for recovery from anesthesia and then were returned to their mothers when stable and allowed to grow in a normal manner. As the animals grow, an aortic coarctation gradually develops. In the control group, a left posterior thoracotomy was performed, but no aortic band was placed.

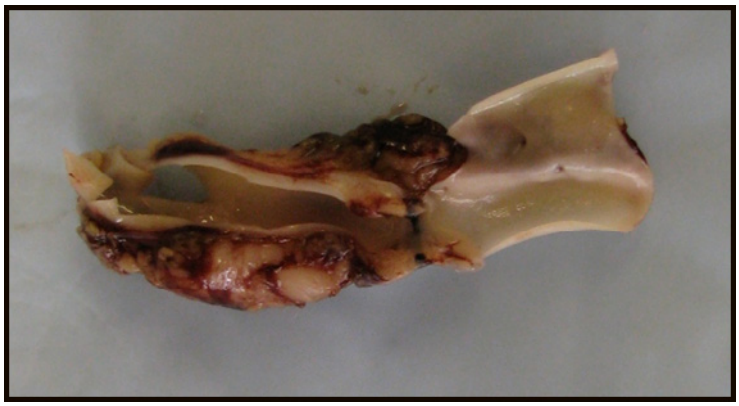

Figure 7. Descending thoracic aorta

At six weeks of age, which is the time point of early failure, hypertrophied and age-matched control animals were euthanized. LV myocardium was frozen in liquid nitrogen and stored at -80° for further analysis.

2. In-vivo Myocardial Function Measurements by Serial Transthoracic Echocardiography

Transthoracic echocardiography was performed weekly (starting at three weeks of age) to monitor LV dimension, wall thickness, and LV cavity volume during the cardiac cycle. To avoid effects of anesthesia or sedatives on non-invasive measurements, animals were conditioned by daily handling. All images were performed without sedation. With this technique, animals remained quiet and still during echocardiographic examination. Transthoracic echocardiography was performed using Sonos 7500 ultrasound machine by Philips equipped with a 12 MHz transducer.

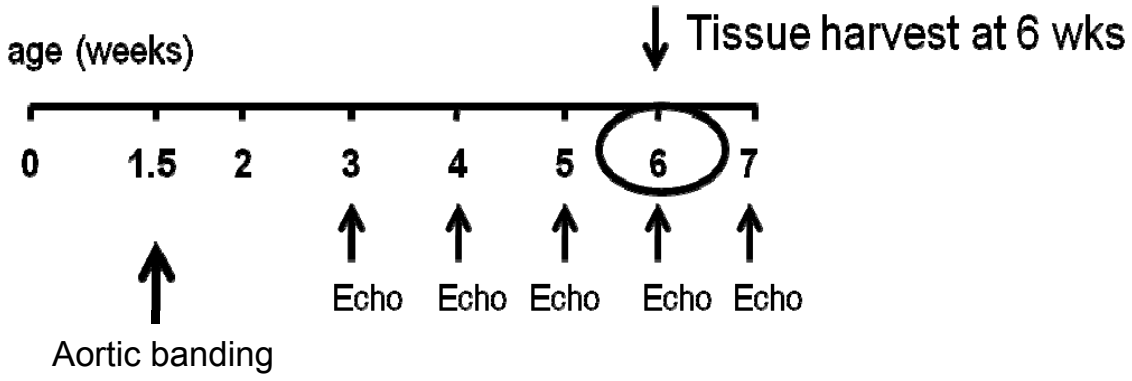

Figure 8. Timeline from aortic banding at 10 days of life to tissue harvest

Starting at three weeks of age, two-dimensional cross-sectional imaging and M-mode echocardiography of LV short axis at the level of the papillary muscles were obtained in aortic banded and control (sham operated) animals.

Measurements of LV mass/volume ratio were used as an indicator for progression of hypertrophy and measurements of the shortening fraction were used as a parameter for contractile function. LV ventricular mass-to-volume ratio (M/V ratio) is determined using dimensions from M-mode echocardiography.

From digitized data, following measurements were obtained by averaging three cardiac cycles:

1) Left ventricular end-diastolic diameter (LV EDD),

2) Left ventricular end-systolic diameter (LV ESD),

3) Left ventricular posterior wall thickness (LV PWD) and

4) RR.

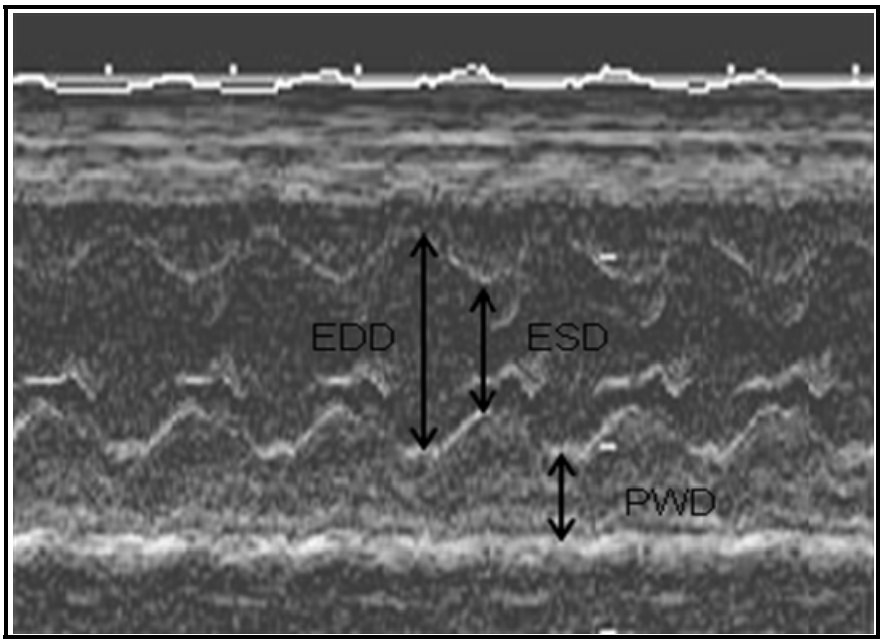

Figure 9. In-vivo myocardial function measurements by 2D transthoracic echocardiography

The following formulae were used for calculation of echocardiographic data:

LV Volume = $3.14*(EDD/2)^2$

LV Mass = $3.14*(EDD/2 + PWD)^2 – 3.14* (EDD/2)^2$

Fractional shortening = (EDD-ESD)/EDD x 100

3. Myocardial Tissue Extraction

(a) RNA Isolation and Quantitation of Nucleic Acids

Total RNA was isolated from frozen LV myocardium (150-200 mg) following a standardized protocol using Trizol Reagent (Invitrogen), which is a mono-phasic solution of phenol and guanidine isothiocyanate.

After washing the RNA pellet twice in 75% ethanol, RNA was diluted in 100-150 µl nuclease free water.

Purity of RNA was assessed by analyzing the 260/280 ratio using Thermo Scientific NanoDrop^{TM} 1000 Spectrophotometer, and RNA integrity was determined by 1% agarose gel electrophoresis.

Optimal absorbance ratio which was used, was 1.8 - 2 (RNA is protein-free).

(b) Protein Isolation

Protein Isolation was performed using a standardized protocol. Ventricular tissue from hypertrophied and control ventricles were pulverized in liquid nitrogen and homogenized in ice-cold buffer containing 150mM NaCl, 20mM Tris-HCl (pH 7.6), 1mM EDTA, 0.5%sodium deoxycholate, 70mM sodium fluoride, 1% Nonidet P-40, 200µM sodium orthovanadate, 2µM phenylmethylsulfonyl fluoride, and complete protease inhibitor cocktail.

(c) Nuclear extraction

A nuclear extract kit from Active Motif (Carlsbad, CA) was used for preparation of nuclear extracts from hypertrophied und control hearts.

4. Immunoblotting

Protein levels of total VEGF, VEGFR-1, sVEGFR-1 and VEGFR-2 were determined by immunoblotting using standard protocols as previously described. Equal protein loading was confirmed by staining of gels with Coomassie brilliant blue. For specific protein detection, the following primary antibodies were used: total VEGF (Millipore, Temecula, MA), VEGFR-2 (Millipore, Temecula, MA), VEGFR-1 (Sigma-Aldrich, St. Louis, MO), and sVEGFR-1 (Zymed Laboratories, San Francisco, CA). Horseradish peroxidase-conjungated antibodies were used as secondary antibodies (GE Healthcare, Piscataway, NJ). The bound antibody was detected by the enhanced chemiluminescence method according to the manufacturer's instruction (GE Healthcare, Piscataway, NJ). After exposure on film, quantitative protein analysis was conducted using laser densitometry. Immunoblotting-data were expressed as arbitrary densitometry units.

5. VEGF Binding ELISA Immunoassay

In order to quantify whether the amount of free, soluble VEGF is decreased in hypertrophied hearts due to binding/trapping by sVEGFR-1, VEGF levels were

measured by a sandwich enzyme-linked immunoassay (ELISA) using Human VEGF Immunoassay (R&D Systems, Minneapolis, MN). LV myocardial samples from hypertrophied and control hearts were homogenized in 20ml of phosphate-buffered saline (PBS) on ice and stored overnight at -20C.

After two freeze-thaw cycles, lysates were centrifuged at 5000g, total protein content was measured and samples of equal protein were loaded onto a microplate, pre-coated with a monoclonal antibody specific for VEGF. Any free, unbound VEGF present in the lysate was bound by the immobilized antibody and detected by incubation with an enzyme-linked polyclonal antibody specific for VEGF after addition of a substrate solution. The developing color was proportional to the amount of VEGF bound in the initial step.

The color development was stopped and the intensity of the color was measured at 450nm and 535nm, respectively. In order to account for optical imperfections in the plate the readings at 535nm were subtracted from readings at 450nm.

6. Immunoprecipitation

Immunoprecipitation with an antibody directed against sVEGFR-1 followed by immunoblotting with anti-VEGF, was performed to demonstrate the binding of VEGF to sVEGFR-1. Ventricular tissue from hypertrophied ventricles was pulverized in liquid nitrogen and homogenized in ice-cold buffer containing 150mM NaCl, 20mM Tris-HCl (pH 7.6), 1mM EDTA, 0.5%sodium deoxycholate, 70mM sodium fluoride, 1% Nonidet P-40, 200μM sodium orthovanadate, 2μM

phenylmethylsulfonyl fluoride (Sigma-Aldrich, St. Louis, MO), and complete protease inhibitor cocktail (Roche, Nutley, NJ).

500µg of total homogenate was immunoprecipitated with 2µg of an antibody directed against sVEGFR-1 (Zymed Laboratories, San Francisco, CA) following the Catch and Release® protocol by Millipore (Millipore, Billerica, MA).

The eluted protein was collected and loaded onto a 10% polyacrylamide gel which was incubated with VEGF primary antibody in 5% milk in TBST at 4°C overnight (Millipore, Billerica, MA) after transfer to a nitrocellulose membrane. After incubation with the secondary antibody, membranes were developed on film using a chemiluminescence kit (GE Healthcare, Piscataway, NJ).

7. Primer Design

Primers are short synthetic oligonucleotides, which are widely used in real time PCR and DNA sequencing. Primers are designed to have a sequence that is the reverse complement of a region of target DNA.

Due to the fact that the rabbit genome is not completely known, an alignment for each gene of interest with the human genome was done using the software Ensemble which is available online at http://www.ensembl.org/index.html. The predicted cDNA was then used for designing primers.

Primer 3 is a software which is developed by Rozen and Skaletsky (Rozen and Skaletsky, 2000 and is available online at http://frodo.wi.mit.edu/).

Below is an example (VEGFR-1 forward primer):

Primer	5`-CTCAACGAGGCAGCATTACA-3`
Template	3`-GAGTTGCTCCGTCGTAATGT-5`
Annealing:	5`-CTCAACGAGGCAGCATTACA-3`
	| | | | | | | | | | | | | | | | | | |
	3`-GAGTTGCTCCGTCGTAATGT-5`

Primers were selected according to the following guidelines: optimal length between 17–28 bases, G+C (Guanin and Cytosin) content between 40 and 60%, melting temperature (T_M) of primers comprised between 55°C and 65°C (the annealing temperature for a primer pair is generally calculated as 5°C lower than the estimated T_M). Further, primers should end with a C or G base within the 3' end (GC clamp). Hairpins (intramolecular interactions) and inverted repeat sequences (like ATATATATAT) should be avoided. All of the selected sequences were further analyzed for additional characteristics (probability of primers forming dimers and/or hairpins) with the computer program Amplify (http://engels.genetics.wisc.edu/amplify/).

Finally, for assessment of gene specificity, all sequences were entered into the Blast software which is available on the National Center for Biotechnology Information website (http://www.ncbi.nlm.nih.gov/). Sequence-specific

oligonucleotide primers were purchased from Operon. All primer sequences are shown in Table 2. A 100μM stock solution was prepared and stored at -20°C. For specific RT-PCR, a 1μM solution was used.

Primer	Sequences	Product Sizes
Total VEGF		301 bp
Forward	CCTTGCCTTGCTGCTCTACC	
Reverse	AGGTTTGATCCGCATGATCTG	
VEGF121		122 bp
Forward	ATCATGCGGATCAAACCTCA	
Reverse	CTCGGCTTGTCACATTTTTC	
VEGF165		122 bp
Forward	ATCATGCGGATCAAACCTCA	
Reverse	CAAGGCCCACAGGGATTTTC	
VEGF189		193 bp
Forward	ATCATGCGGATCAAACCTCA	
Reverse	CAAGGCCCACAGGGAACGCT	
VEGFR-1		186 bp
Forward	CTCAACGAGGCAGCATTACA	
Reverse	CTGCTTGTGGAACTCATCCA	
sVEGFR-1		134 bp
Forward	GAACCTGCTCCTCAAGAACG	
Reverse	CCTTTTTGTTGCAGTGCTCA	
VEGFR-2		235bp
Forward	CAAGTGCATCCACAGAGACCTG	
Reverse	GGAAAATATCTCCCAGAGCAACAC	
GAPDH		213bp
Forward	AGGTCATCCACGACCACTTC	
Reverse	AGGCCATGCCAGTGAGTTTC	

Table 2. Primer sequences and their product sizes

8. Gradient PCR

Gradient PCR is a technique that is used to determine the optimal annealing temperature in a PCR reaction for the gene of interest. The PCR machine was set in such a way that the wells in the thermo cycle block are heated from 50° to

62°C. The same master mix as for RT-PCR was used in order to mimic PCR conditions.

PROTOCOL FOR GRADIENT PCR
(1) Incubate at 48.0°C for 1h
(2) Incubate at 94.0°C for 10 min
(3) Incubate at 94.0°C for 15 sec
(4) Gradient from 50° to 62°C for 30 sec
(5) Incubate at 72°C for 45 sec
(6) Plate Read
(7) Go to line 3 for 40x
(8) Melting Curve from 62°C to 95°C, read every 0.2°C, hold for 2 sec
(9) Incubate at 4°C forever

Table 3. Protocol for Gradient PCR

9. Agarose Gel Electrophoresis

Electrophoretic analysis of gradient PCR products was performed using a 1% agarose gel.

The brightest band determined the optimal melting temperature. The gel was run at 100V for 1hour, and ethidium bromide was added for visualization.

Lanes	1	2	3	4	5	6	7	8	9	10	11	12
Temp.	50°	50.3°	51.1°	52°	53.4°	55.2°	57.2°	58.9°	60.2°	61.1°	61.8°	62°

Table 4. Lane layout for gradient on agarose gel electrophoresis

10. Quantitative RT-PCR

(a) RT-PCR – General Principles

Reverse transcription polymerase chain reaction (RT-PCR) is used to amplify a defined piece of a RNA molecule. This method allows exponential amplification of short DNA sequences within a longer double stranded DNA molecule. mRNA is first transcribed into cDNA (complementary DNA) using dNTPs and reverse transcriptase. The polymerase chain reaction (PCR) then amplifies cDNA using the enzyme DNA polymerase.

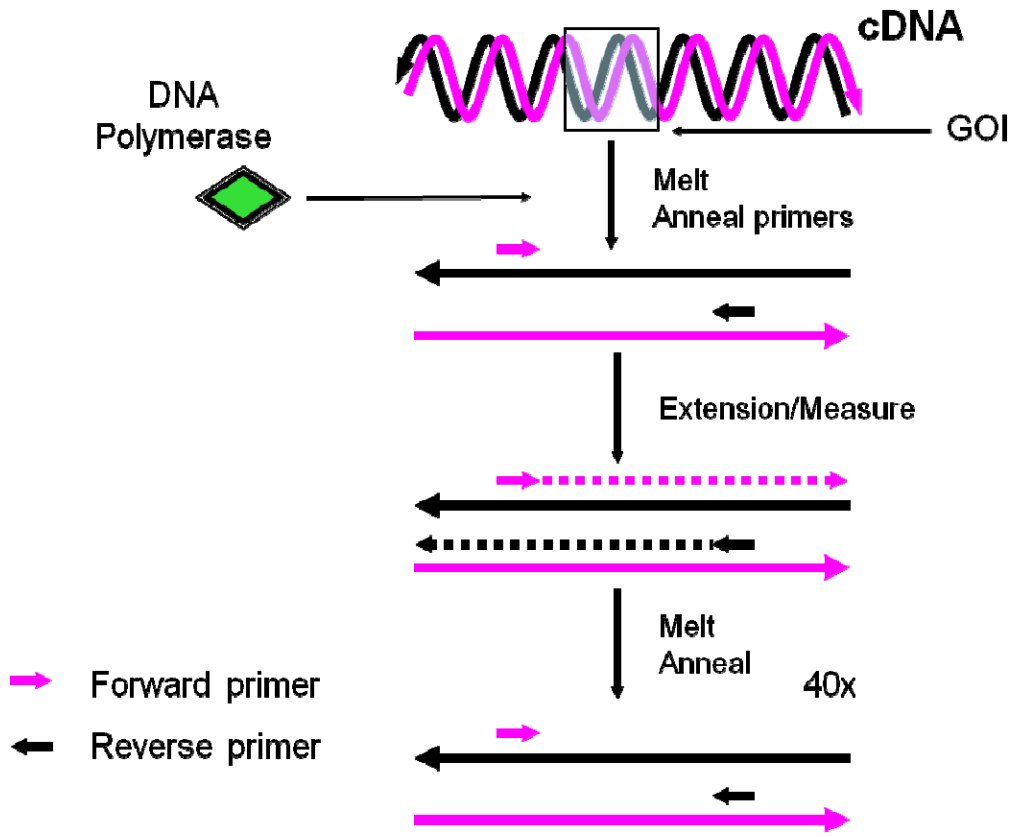

Figure 10. PCR principle. One PCR cycle is shown, which is repeated for 40 times (modified after Stratgene power point presentation)

Heating of the reaction up to 95°C melts the two DNA strands apart, whereas at lower temperatures, specific primers are annealed. Raising the temperature up to 72°C induces the DNA polymerase to extend the DNA.

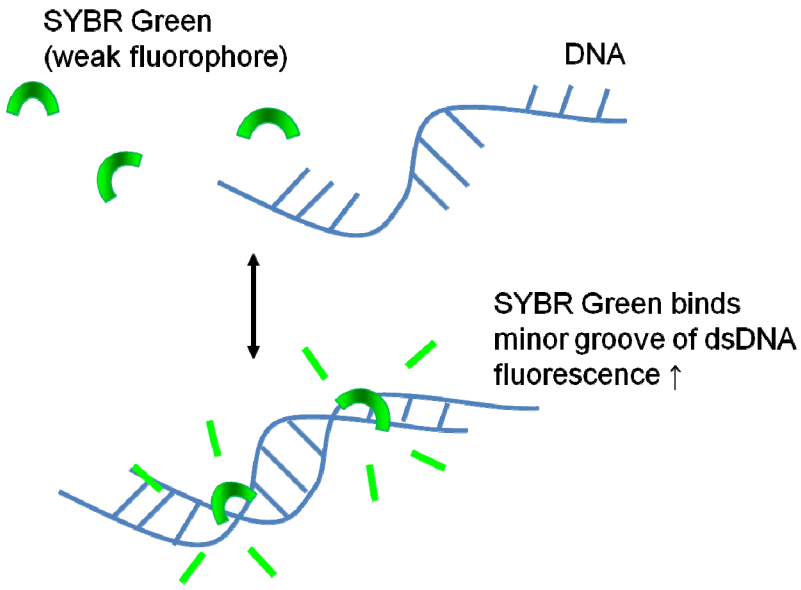

Figure 11. SYBR green dye – mechanism (modified after Stratagene power point presentation)

SYBR Green is a dye that was used to monitor DNA synthesis. SYBR Green binds to the minor grove of double stranded DNA (dsDNA). This resulting complex absorbs blue light (wavelength = 488 nm) and emits green light (522 nm) as shown in Figure 11.

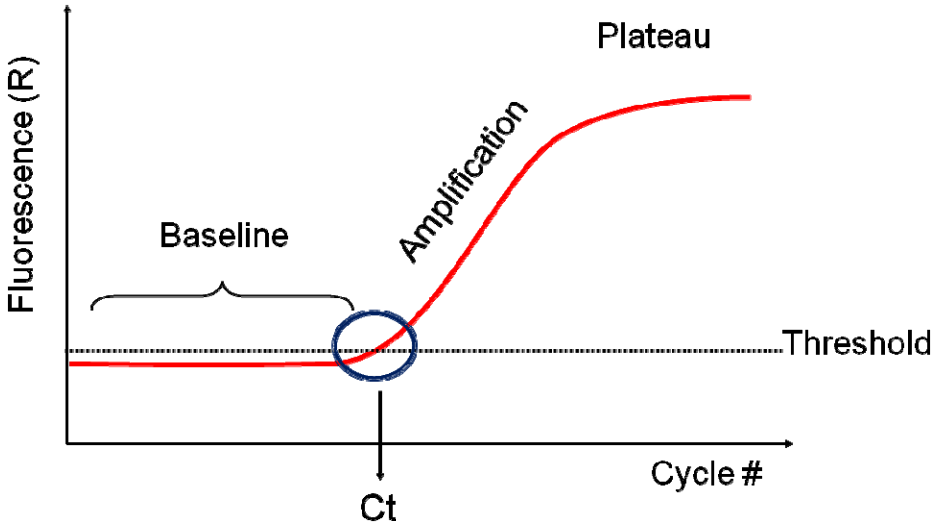

Figure 12. Typical PCR amplification plot. Each reaction was run in triplicates. We calculated the Ct value (Threshold Cycle), which is a fractional PCR cycle number at which the fluorescence intensity crosses the established threshold line

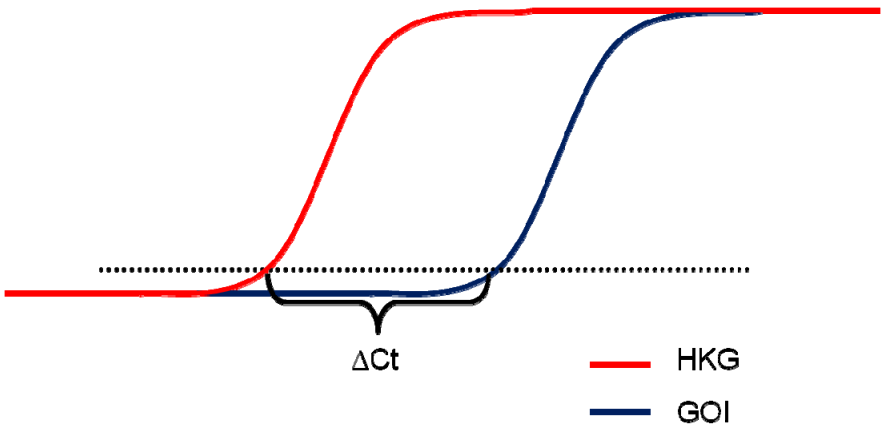

Figure 13. PCR curves of the HKG and GOI

In addition to the gene of interest (GOI), glyceraldehyde-3-phosphate dehydrogenase (GAPDH) and 18S were used as a reference gene (housekeeping gene, HKG).

Comparative quantification was determined using the ΔΔ Ct Method, according to the following formula:

$$\Delta\Delta Ct=(Ct\ GOI_{\ Control} - Ct\ HKG_{\ Control}) - (Ct\ GOI_{\ Hypertrophy} - Ct\ HKG_{\ Hypertrophy})$$

(b) Current experiment – qRT-PCR

SYBR® Green qRT-PCR was used to quantify mRNA expression levels of total VEGF, VEGF isoforms (121, 165, and 189) and the VEGF receptors (VEGFR-2, VEGFR-1 and sVEGFR-1), GLUT1 and GLUT4.

For normalization, GAPDH (Glyceraldehyde 3-phosphate dehydrogenase) was used as a reference gene which was compared to 18S classic as additionally internal control (Ambion). SYBR® Green two-step RT-PCR using the ABI PRISM® 7700 Sequence Detection System (Applied Biosystems Inc) was used to quantify mRNA expression levels of total VEGF, all VEGF isoforms (121, 165 and 189), and VEGFR-2. Briefly, purification of poly A^+ RNA from total RNA was achieved following the Oligotex mRNA Batch Protocol (Qiagen). RETROscript kit (Ambion) was applied to transcribe 5µl mRNA in a final reaction volume of 20µl at 44ºC for 59 min and 52ºC for 10 min using MMLV reverse transcriptase. cDNA samples were diluted 6 times with nuclease-free water (Ambion) and stored at -20ºC until

further use. Sequence-specific oligonucleotide primers were purchased from Invitrogen. A common VEGF forward primer was previously designed based on the fact that all VEGF isoforms share exon one to five. The various reverse primers were designed to amplify each isoform using its specific sequence mode. All primer sequences are shown in Table 2. Quantification of mRNA expression levels for VEGFR-1 and sVEGFR-1 was performed with a one-step method using iScript™ One-Step RT-PCR Kit with SYBR® Green (BioRad).

Reaction Mix for One-Step qRT-PCR
25 µl SYBR Green
5 µl forward primer
5 µl reverse primer
1 µl reverse transcriptase
5 µl RNA (100ng/rxn)
9 µl Nuclease-Free Water

Table 5. Reaction mix for qRT-PCR

PCR amplification was performed in a final volume of 50µl containing 5µl of RNA (100ng/rxn) and 25µl of SYBR® Green. Primers were purchased from Operon. To determine the optimum annealing temperature (53.4°C) for subsequent qRT-PCR, 1% agarose gels with temperature gradients were analyzed. After an initial

denaturation at 94°C for 10 min, a 2-step cycle procedure was performed (denaturation at 94°C for 15s, annealing and extension at 53.4ºC for 30 seconds) for 50 cycles in a PTC-200 Peltier thermal cycler and Chromo 4 continuous fluorescence detector (MJ Research). Each of the samples was run in triplets. A gradient inclusive melting curve was run for primer optimization. Fluorescence representing each gene was normalized to GAPDH mRNA content using the REST© software.

PROTOCOL FOR ONE-STEP qRT-PCR
(1) Incubate at 48.0°C for 1h
(2) Incubate at 94.0°C for 10 min
(3) Incubate at 94.0°C for 15 sec
(4) Incubate at 53.4°C for 30 sec
(5) Incubate at 72°C for 45 sec
(6) Incubate at 78°C for 1 sec
(7) Plate Read
(8) Go to line 3 for 40x
(9) Melting Curve from 62°C to 95°C, read every 0.2°C, hold for 2 sec
(10) Incubate at 4°C forever

Table 6. Protocol for qRT-PCR

11. Melting (Dissociation) Curve

SYBR Green is able to detect any double stranded (ds) DNA including primer dimers, contaminated or genomic DNA. In order to ensure that the specific product, the gene of interest, is amplified, it is necessary to run a melting curve. Therefore, at the end of each amplification reaction, the PCR machine is programmed to run a melting curve (also known as dissociation curve).

All products generated during the PCR amplification reaction are melted at 96°C and then subsequently annealed at 55°C. Melting of dsDNA causes a dissociation of SYBR green from the DNA and fluorescence decreases. These changes in fluorescence are measured every 0.2°C. As a result, changes in fluorescence are plotted against temperature.

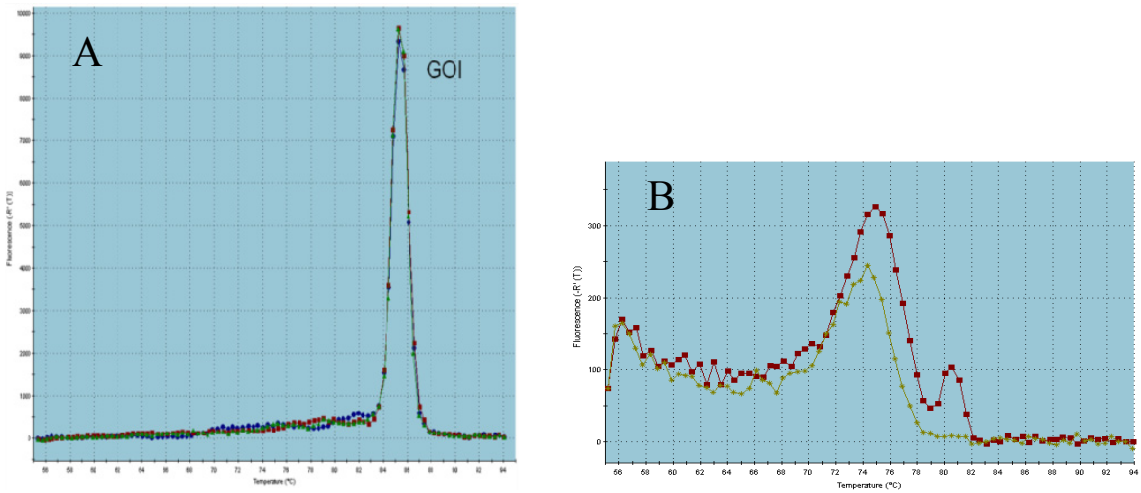

Figure 14. Melting curves. A shows a nicely shaped melting curve; B is indicative for primer dimers

Ideally, the plot shows a single peak within the range of 80-90°C (*Figure 14A*). Secondary peaks or shoulders, as indicated in *Figure 14B*, are indicators that something other than the gene of interest is present among the reaction products.

12.Blocking of sVEGFR-1 by Treatment with Placental Growth Factor (PlGF)

a) Principle and Timeline

PlGF stimulates angiogenesis by enhancing VEGF signaling by ligand shifting (29). The growth factor displaces VEGF from VEGFR-1/sVEGFR-1, and thereby allows it to activate VEGFR-2, which is the main mediator of VEGF-induced angiogenesis.

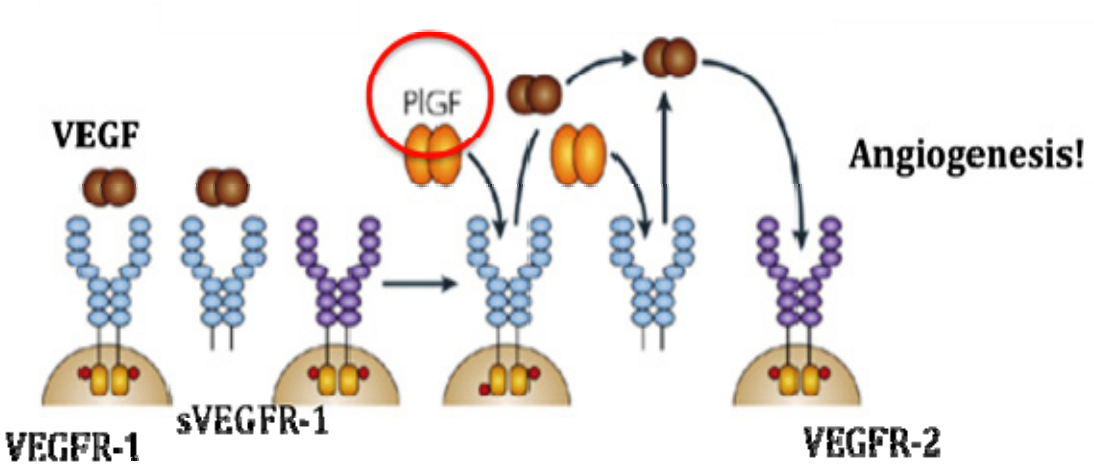

Figure 15. Mechanism of PlGF binding to VEGFR-1/sVEGFR-1

Based on this concept, we treated hypertrophied hearts with placental growth factor (PlGF), a ligand specifically binding to VEGFR-1 and not VEGFR-2. 2μg/kg recombinant human PlGF protein (R&D Systems Inc., Minneapolis, MN) were injected into the pericardium to maximize local availability and minimize systemic side effects, twice, at 4 weeks of age (compensated hypertrophy) and again at 6 weeks of age (early failure).

Animals were followed weekly by echocardiography in order to monitor ventricular function and contractility.

At 7 weeks of age, animals were euthanized and tissue was harvested for further analysis. Tissue samples were then used to determine free, unbound VEGF using the same ELISA described above.

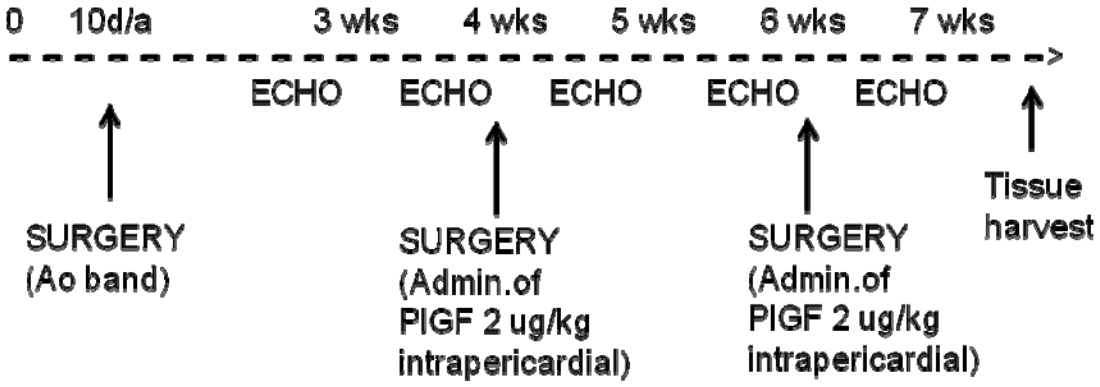

Figure 16. Timeline and administration of PlGF

b) Determination of Capillary Density

LV cross-sections were obtained from control, hypertrophied hearts and PlGF treated hypertrophied hearts. Cross-sections of the left ventricle were fixed in 4% paraformaldehyde/PBS and paraffin-embedded cut into 10-μm thick slices. The sections were de-paraffinized and cardiomyocytes were stained with desmin (Epitomics Inc, Burlingame, CA) and a red-fluorescent secondary antibody (Alexa-594^{TM}fluorophore, Invitrogen, Carlsbad, CA) at a concentration of 1:200. Capillaries were stained with CD31 (Dako Corporation, Carpinteria, CA) at a concentration of 1:5 in 5% fetal serum in PBS, pH 7.4 followed by incubation with a green fluorescent secondary antibody (Alexa-488 fluorophore, Invitrogen, Carlsbad, CA).

Nuclei were stained with blue fluorescent 4', 6-diamidino-2-phenylindole (DAPI) nucleic acid stain (Invitrogen, Carlsbad, CA). Cover-slips were applied to the sections with fluorescent mounting medium (Dako Corporation, Carpinteria, CA). Slides were visualized using an Axiovert 35 Microscope (Carl Zeiss, Jena, Germany) with a Nikon 20x objective (NA = 10x/0.75).

Microvascular density was determined on 15 different, randomly selected fields from each slide (6 sections per group). Within a calibrated graticule, all vessels identified by the computer software/image analyzer were counted using the MetaMorph® Imaging System software. (Universal Imaging Corporation, West Chester, PA).

13. Animal Care

All animals received humane care from the Animal Resources of Children's Hospital Boston and the investigations were accordance with the "Guide for the Care and Use of Laboratory Animals" prepared by the National Academy of Sciences and published by the US National Institutes of Health (NIH Publication No. 85-23, revised 1996). The protocol was reviewed and approved by the Institutional Animal Care and Use Committee at Children's Hospital Boston.

14. Statistical Analysis

Data were analyzed using SPSS software package (version 11.0, SPSS Inc., Chicago, IL) and are reported as mean±standard error of the mean (SEM). A two-tailed unpaired Student's t-test was used for comparison between groups if normality was passed. A value of $p \leq 0.05$ was considered statistically significant.

Results

RESULTS

1. Echocardiographic Results

a. Left Ventricular Mass/Volume (M/V) ratio

Left ventricular mass to left ventricular cavity volume measurement is an indicator of progression of hypertrophy to failure and was calculated based on echocardiographic measurements for control and hypertrophied hearts. In control hearts, there is no change in the mass-to-volume ratio.

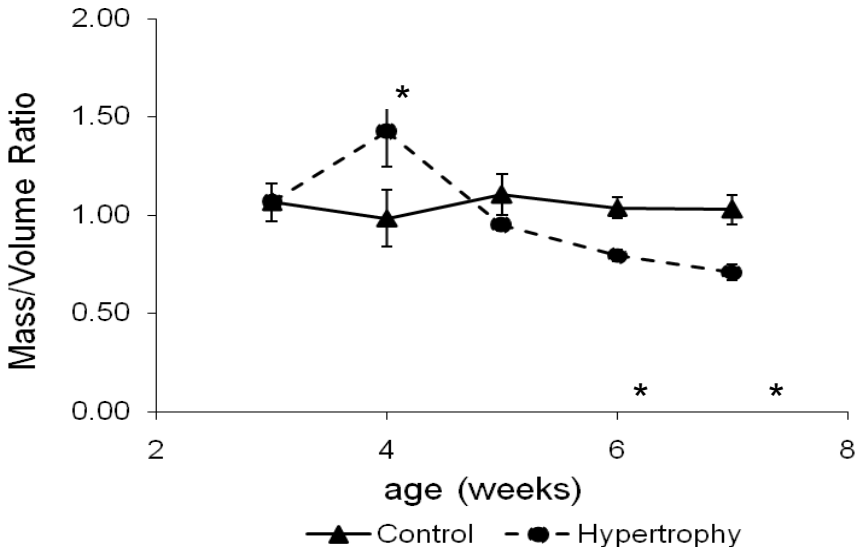

Figure 17. M/V ratio of control and hypertrophied hearts. *p<0.05 vs control

In hypertrophied hearts, M/V ratio was significantly increased at four weeks of age, followed by a significant decline at six weeks of age, indicating ventricular

dilatation. Data in the graph below are expressed as mean±SEM ($p<0.05$ versus Controls).

b. Contractile function determined by Shortening Fraction

In this study, the shortening fraction (%SF) was used as an indicator of contractile function. Figure 18 shows shortening function was conserved in control hearts, however, in hypertrophied hearts we noticed a significant decrease in contractile function starting at 4 wks of age.

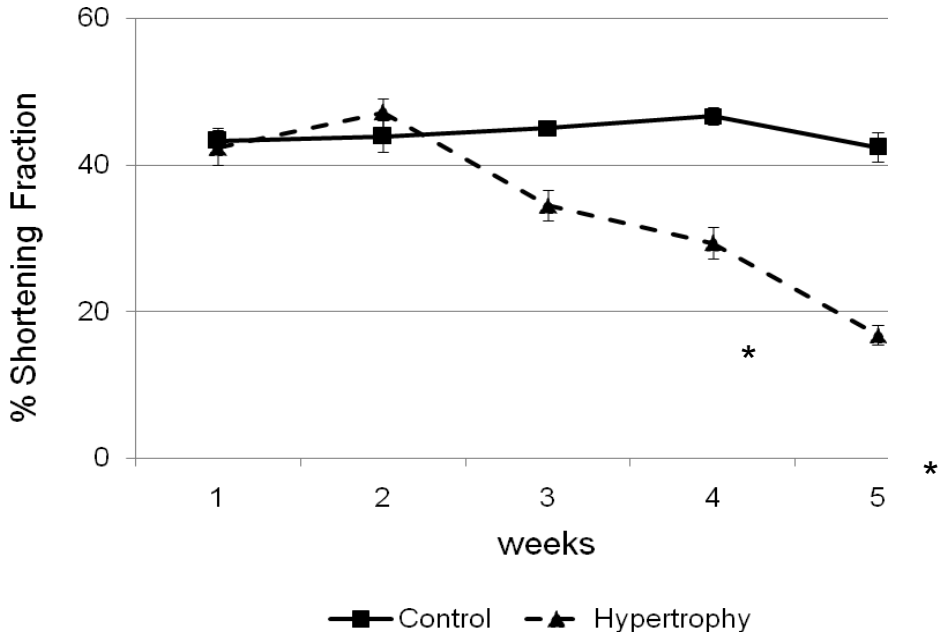

Figure 18. Shortening fraction.*p<0.05 versus control

2. Reference genes used for qRT-PCR

For qRT-PCR, GAPDH and 18S were used as a reference gene. Representative gels depicting both reference genes (GAPDH and 18S) are shown. Both reference genes are unchanged in hypertrophied myocardium at the onset of failure. At this time point these genes can be used as reference for analysis for qRT-PCR.

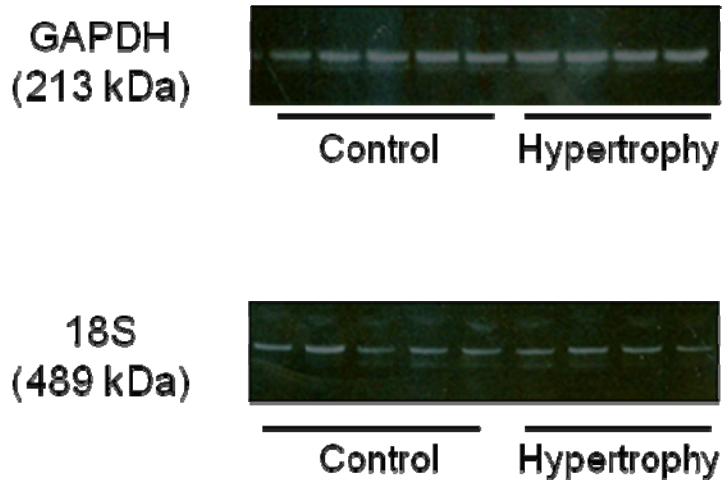

Figure 19. Reference genes GAPDH and 18S used for qRT-PCR

3. VEGF Isoforms – Results on Transcriptional and Translational Level

The vascular endothelial growth factor (VEGF) is the most important inducer of angiogenesis in the heart. VEGF121, VEGF165 and VEGF189 are isoforms present in the heart. In the current study, we looked on protein and mRNA level for all VEGF isoforms.

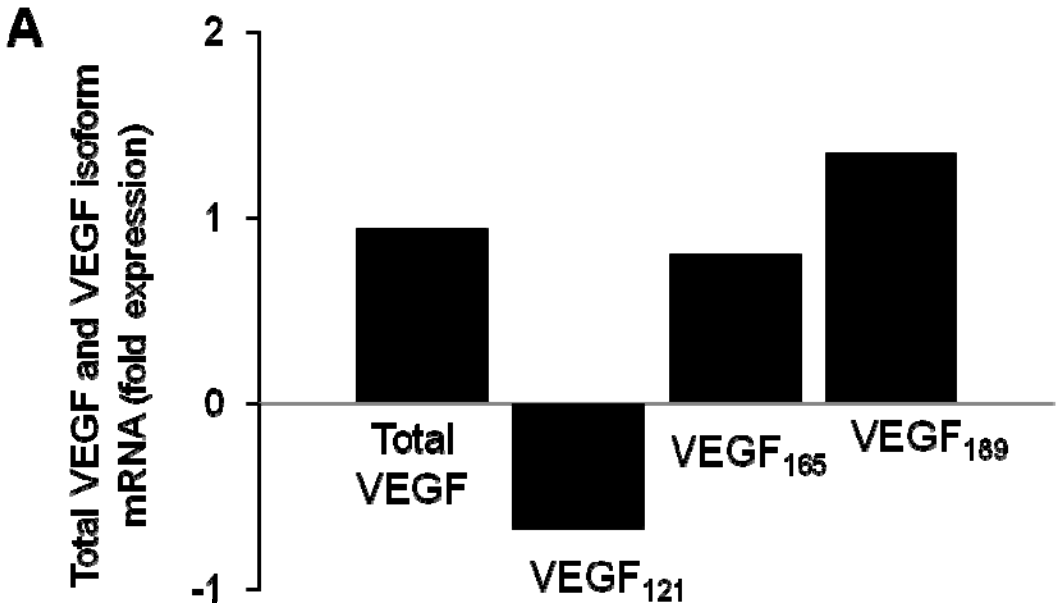

Figure 20. Total VEGF and VEGF Isoform mRNA expression levels

mRNA levels of total VEGF, VEGF isoforms 121, 165 and 189 are summarized in the bar graph below (A).

There was no significant difference between hypertrophied and control hearts.

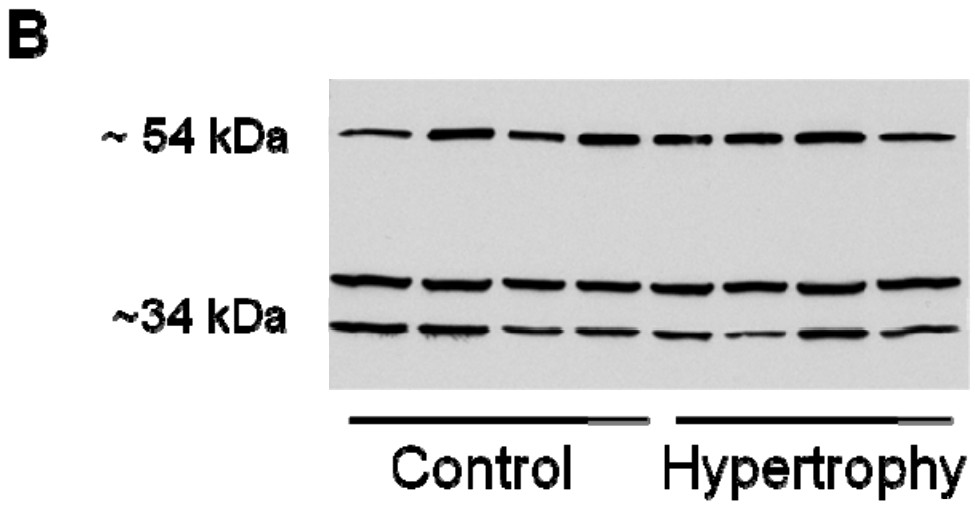

Figure 21. Representative immunoblot for total VEGF

(B) shows a representative immunoblot for total VEGF and (C) the summary of all densitometry data is depicted in the graph below. Data are expressed as mean±SEM. Corresponding to the mRNA results, protein levels are not different between control and hypertrophied myocardium.

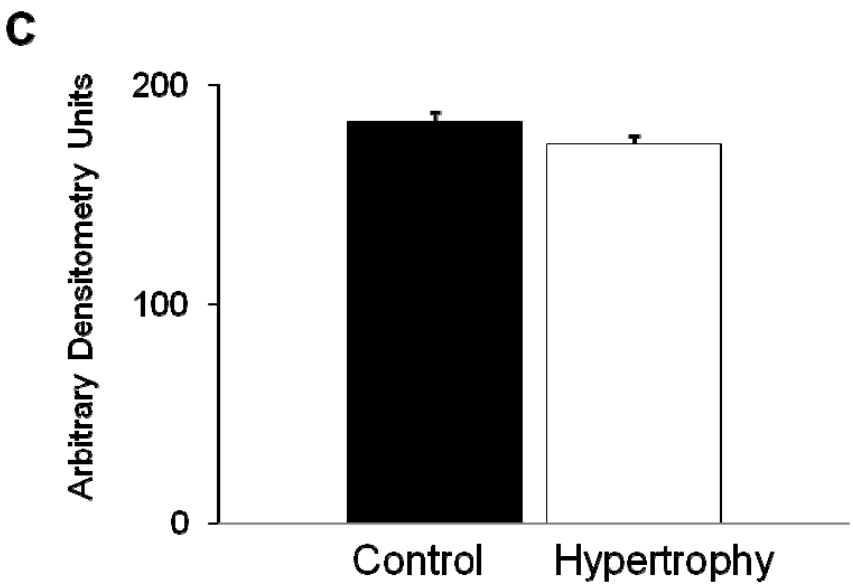

Figure 22. Summary of all densitometry data for total VEGF

4. VEGF Receptors – Relative mRNA expression and representative immunoblots

a. Relative mRNA expression for VEGF Receptors

Relative expression of mRNA of VEGFR-2, VEGFR-1 and sVEGFR-1 between control and hypertrophied hearts is indicated by the first bar graph. There was no difference of the angiogenesis-promoting receptor VEGFR-2 between hypertrophied and control hearts. In comparison, VEGFR-1 (*p=0.001) and the soluble VEGFR-1 (*p=0.001) mRNA levels were significantly (7-fold) up-regulated in hypertrophied hearts compared to age-matched control hearts.

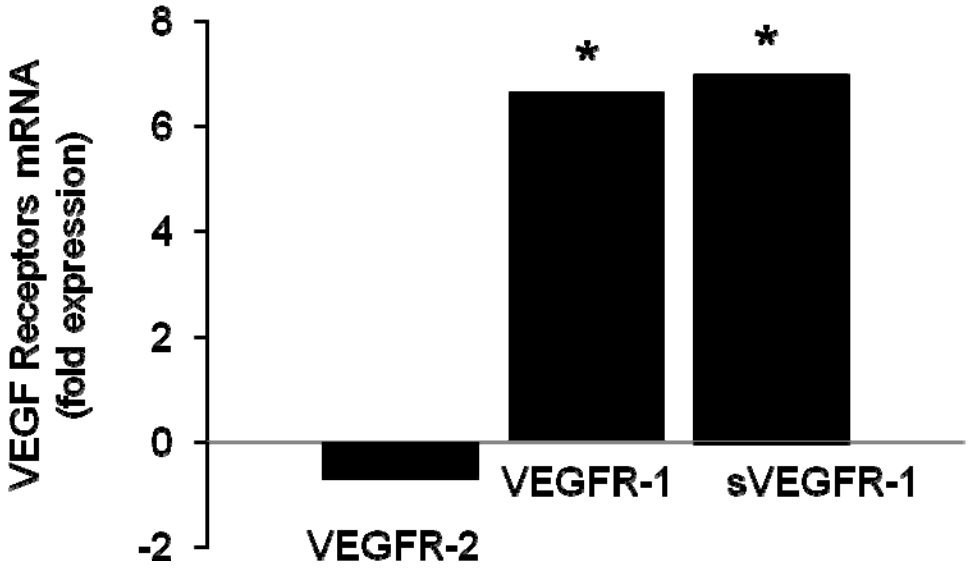

Figure 23. mRNA expression levels of VEGFR-1, VEGFR-1 and sVEGFR-1

b. Protein levels for VEGFR-1 and sVEGFR-1

A representative immunoblot on top of the following graph and the summary of all densitometry data (mean±SEM) are shown for VEGFR-1. Protein levels of the membrane-bound VEGFR-1 are significantly up-regulated in hypertrophied myocardium (*p=0.031).

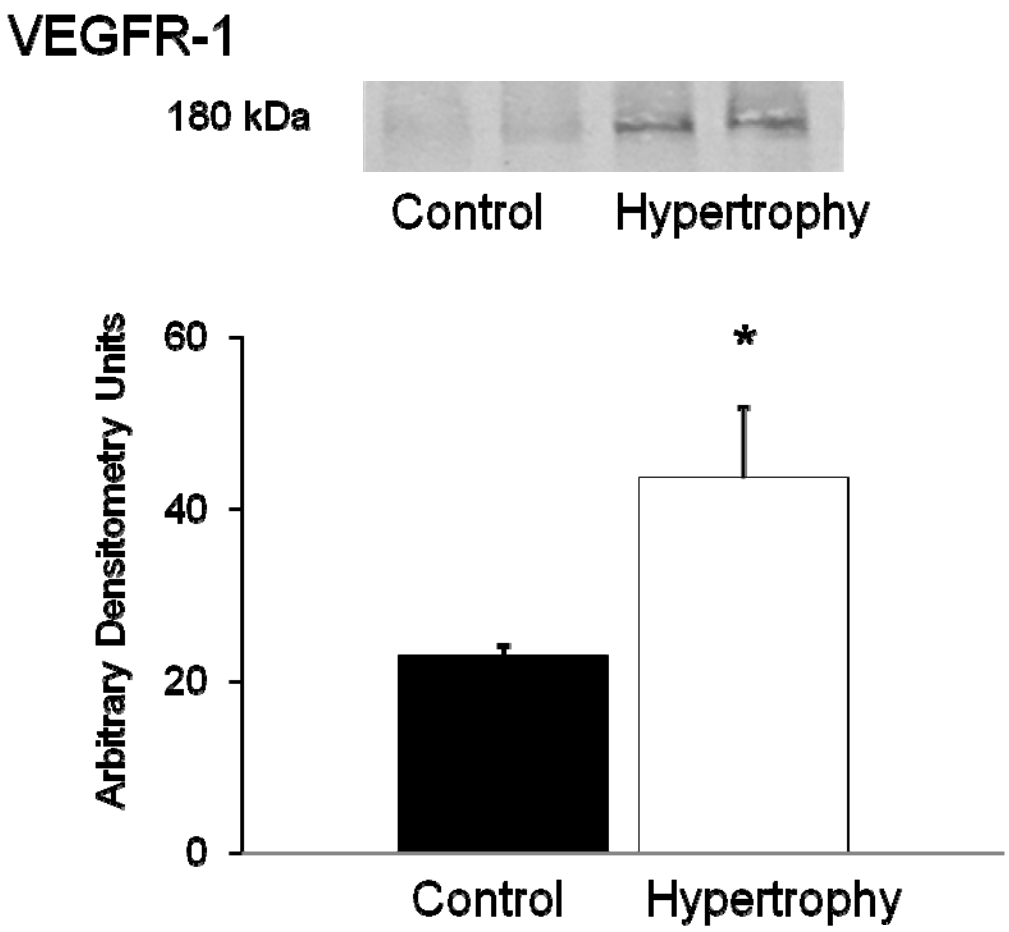

Figure 24. A representative immunoblot and a summary of all densitometry data for VEGFR-1

The following bar graph shown for soluble VEGFR-1 depicts cumulated data from six samples per group and data are expressed as mean±SEM.

sVEGFR-1 protein levels corresponding to the mRNA levels are significantly up-regulated in hypertrophied myocardium (*p=0.016).

A representative immunoblot of sVEGFR-1 is shown as well.

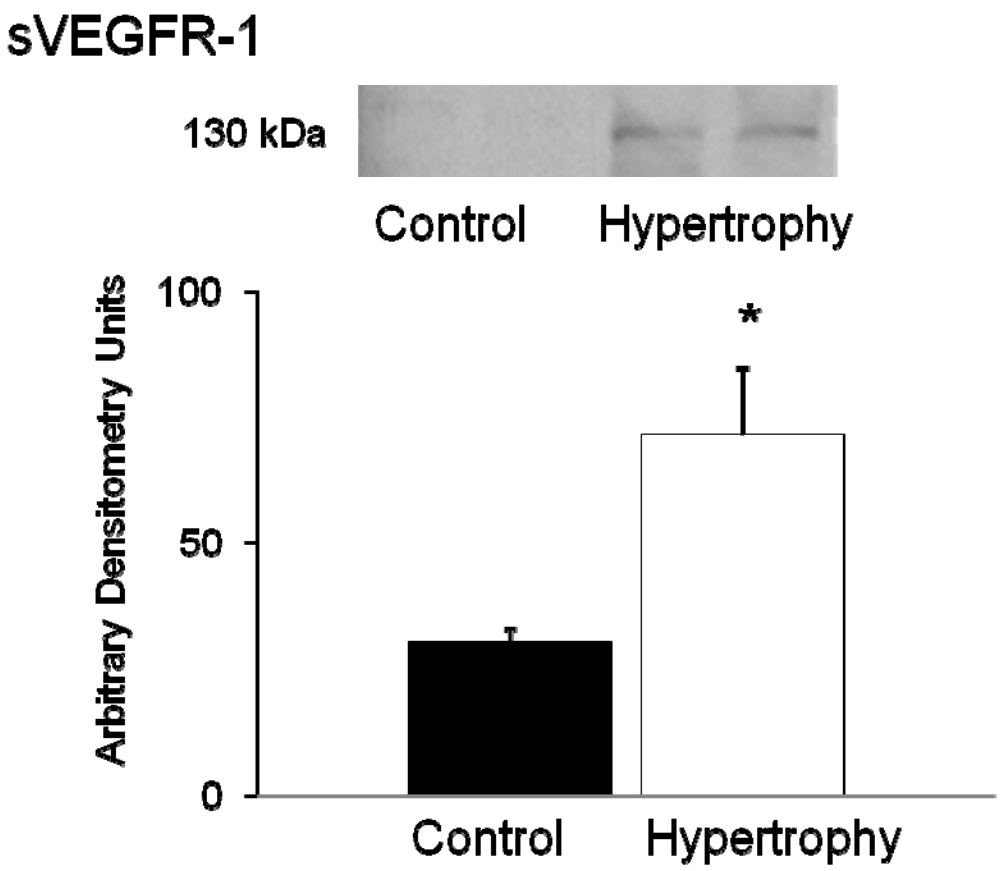

Figure 25. Protein levels for soluble VEGFR-1

c. Protein levels for VEGFR-2

In contrast to VEGFR-1, protein levels of the angiogenesis promoting receptor, VEGFR-2, were unchanged in hypertrophied versus control hearts. A representative immunoblot and the summary of all densitometry data are shown below.

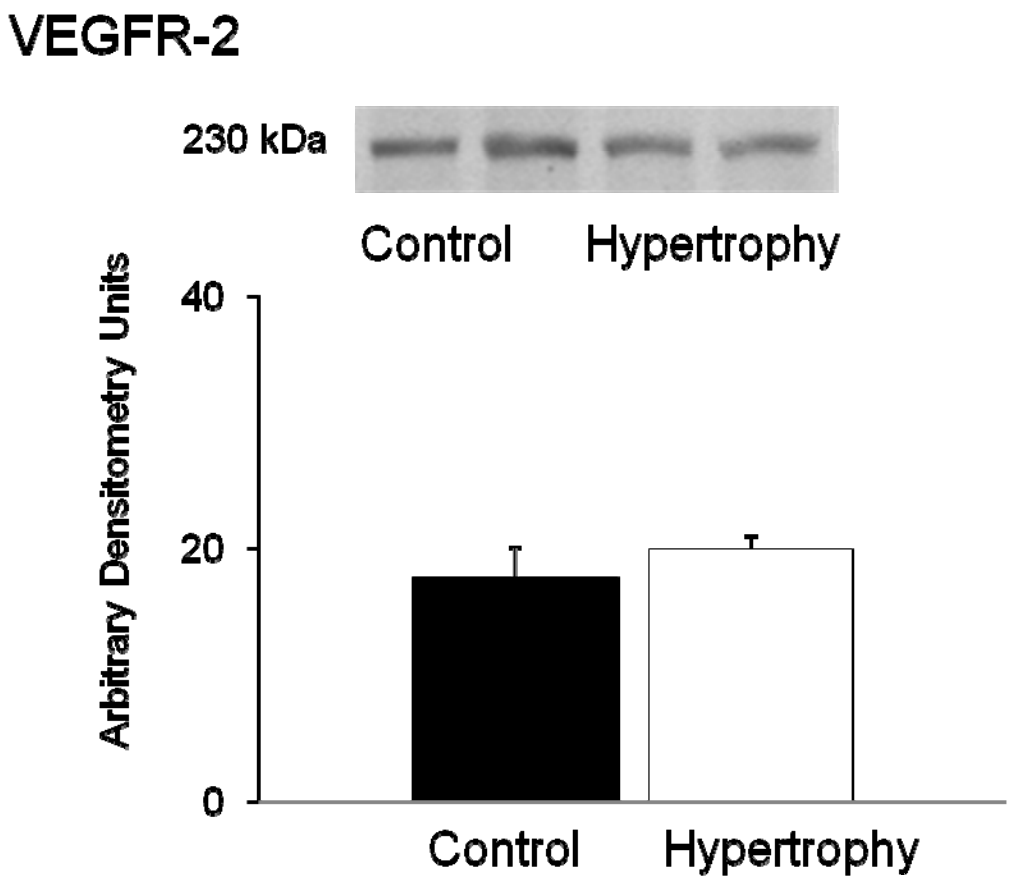

Figure 26. Protein levels for the angiogenesis stimulating receptor, VEGFR-2

5. Binding of VEGF to sVEGFR-1

sVEGFR-1 immunoprecipitated tissue lysates from hypertrophied myocardium were blotted against VEGF and a representative immunoblot is shown. These results demonstrate the binding of VEGF to sVEGFR-1 (A). The immunoblots were also blotted against the immunoprecipitating antibody directed against sVEGFR-1 indicating equal loading (B).

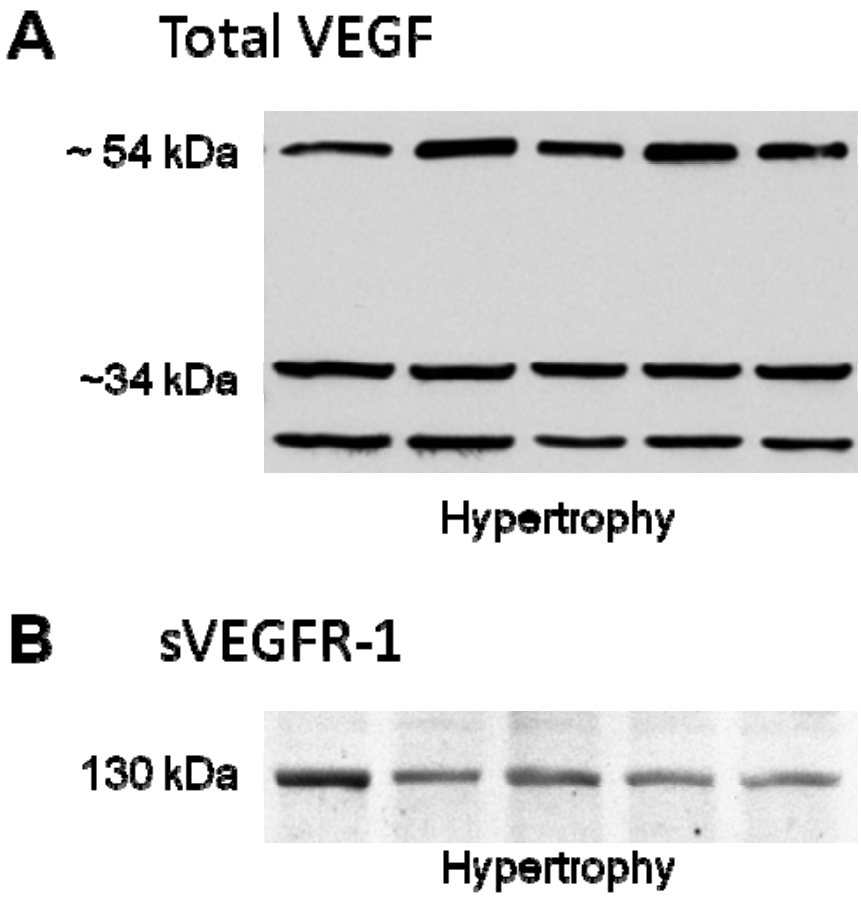

Figure 27. Binding of VEGF to sVEGFR-1

Free, soluble VEGF protein levels were measured by ELISA in tissue lysates obtained from hypertrophied and control hearts. Hypertrophied hearts showed decreased levels of free, soluble VEGF in comparison to control hearts ($p=0.03$), indicative of a significantly higher amount of VEGF bound to sVEGFR-1. Data are expressed as mean±SEM.

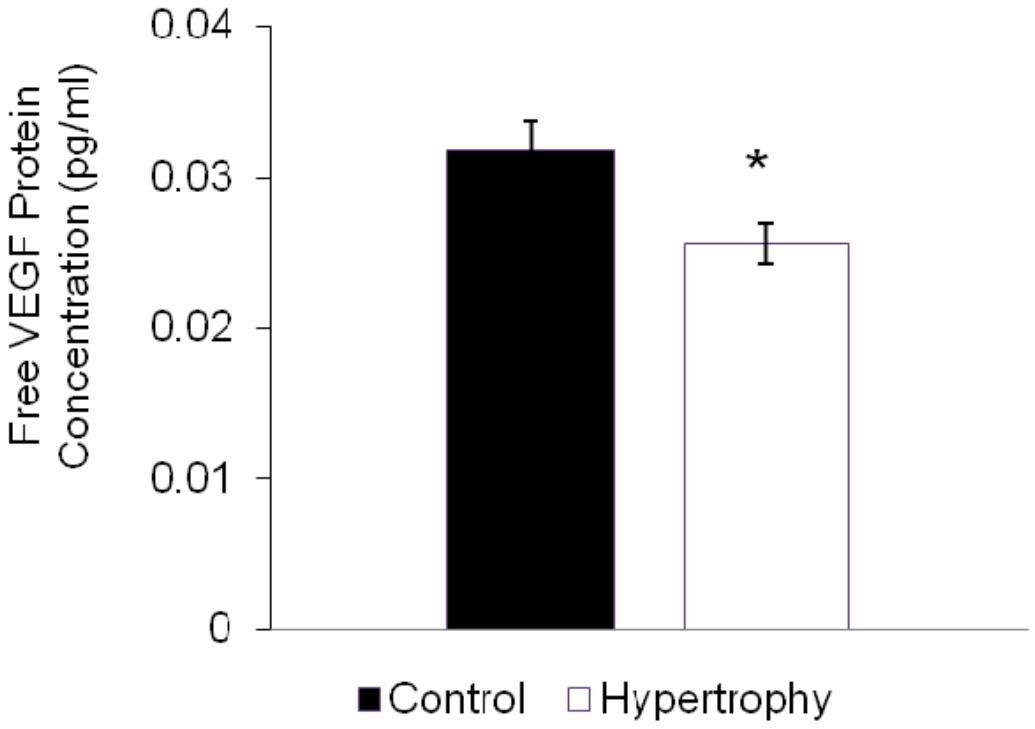

Figure 28. Free VEGF Protein concentration in control and hypertrophied myocardium

6. Sequence-specific primers and sizes of amplicons generated for qRT-PCR

Primer	Sequences	Product Sizes
Total VEGF		301 bp
Forward	CCTTGCCTTGCTGCTCTACC	
Reverse	AGGTTTGATCCGCATGATCTG	
VEGF121		122 bp
Forward	ATCATGCGGATCAAACCTCA	
Reverse	CTCGGCTTGTCACATTTTTC	
VEGF165		122 bp
Forward	ATCATGCGGATCAAACCTCA	
Reverse	CAAGGCCCACAGGGATTTTC	
VEGF189		193 bp
Forward	ATCATGCGGATCAAACCTCA	
Reverse	CAAGGCCCACAGGGAACGCT	
VEGFR-1		186 bp
Forward	CTCAACGAGGCAGCATTACA	
Reverse	CTGCTTGTGGAACTCATCCA	
sVEGFR-1		134 bp
Forward	GAACCTGCTCCTCAAGAACG	
Reverse	CCTTTTTGTTGCAGTGCTCA	
VEGFR-2		235bp
Forward	CAAGTGCATCCACAGAGACCTG	
Reverse	GGAAAATATCTCCCAGAGCAACAC	
GAPDH		213bp
Forward	AGGTCATCCACGACCACTTC	
Reverse	AGGCCATGCCAGTGAGTTTC	

Table 7. Sequence-specific primers and sizes of amplicons

7. Treatment with Placental Growth Factor (PlGF)

a. Echocardiographic results:

Left ventricular Mass/Volume (M/V) ratio

M/V ratio is an indicator of progression of hypertrophy. Figure 13 shows M/V ratio of control, hypertrophied and PlGF-treated hypertrophied myocardium. PlGF preserved adaptive hypertrophied growth of the LV indicated by a significant increase starting at 4 weeks of age. Hypertrophied animals, however, underwent peak hypertrophy at 4 weeks of age and subsequently went into failure at six weeks of age.

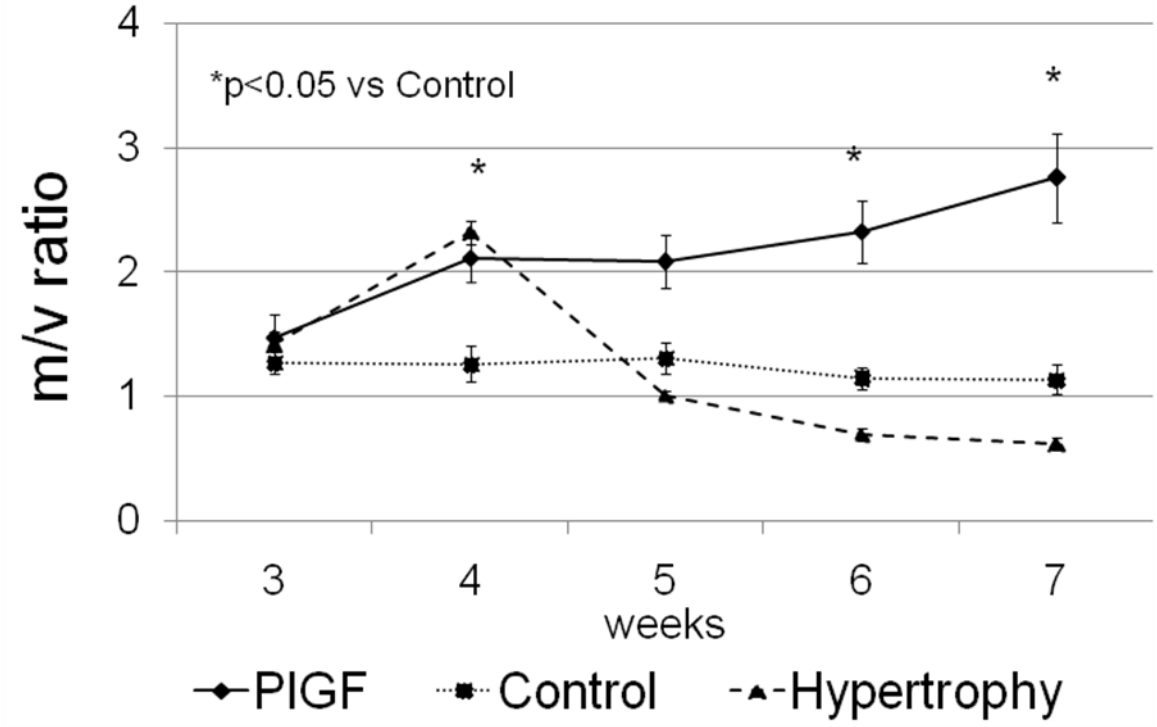

Figure 29. Mass/Volume Ratio of control, hypertrophied and PlGF-treated hypertrophied hearts (*p<0.05,±SEM, n=4-7)

Shortening Fraction (%SF)

Shortening Fraction, a parameter of contractile function, is preserved in PIGF animals throughout the observation period.

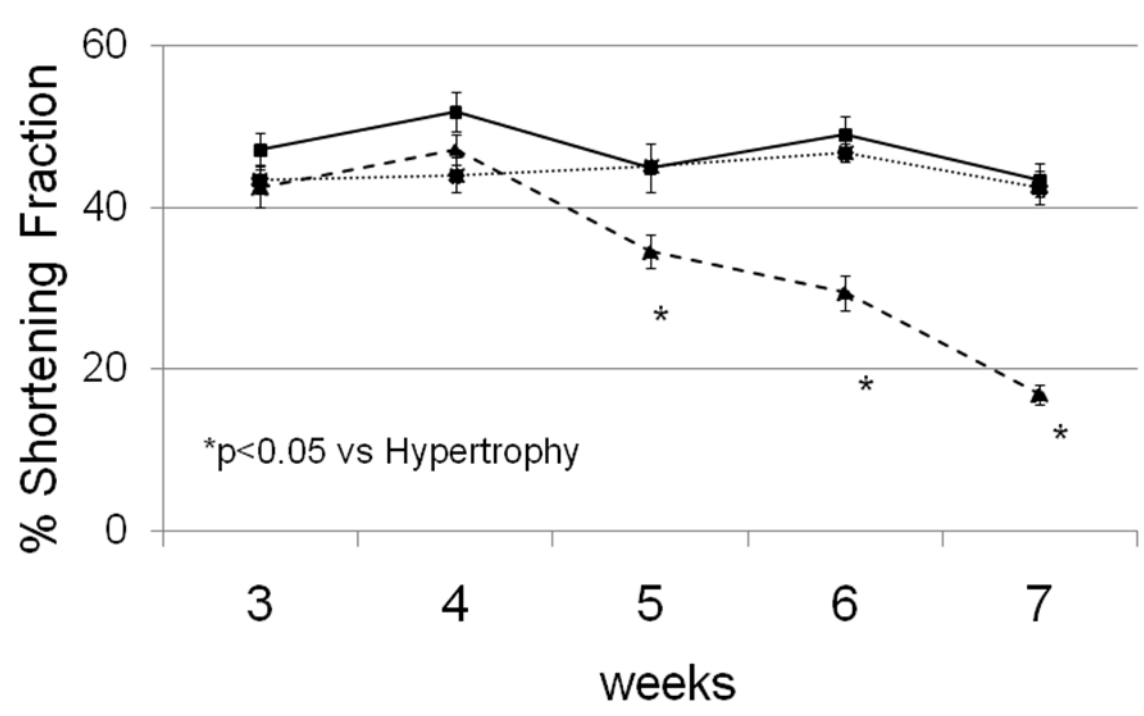

Figure 30. Shortening fraction (%SF)

b) Capillary Density

Increased myocardial VEGF levels resulted in capillary growth. We have previously shown that increasing VEGF levels results in capillary growth and preserves contractile function despite the presence of increased pressure loading on the ventricle.

In the presence of the sVEGFR-1 inhibitor PlGF, more endogenous VEGF is available to induce capillary growth.

Therefore, we determined capillary density in hypertrophied myocardium compared to hypertrophied myocardium with PlGF present.

There was a significant increase in the number of capillaries expressed per number of nuclei following inhibition of sVEGFR-1 with PlGF.

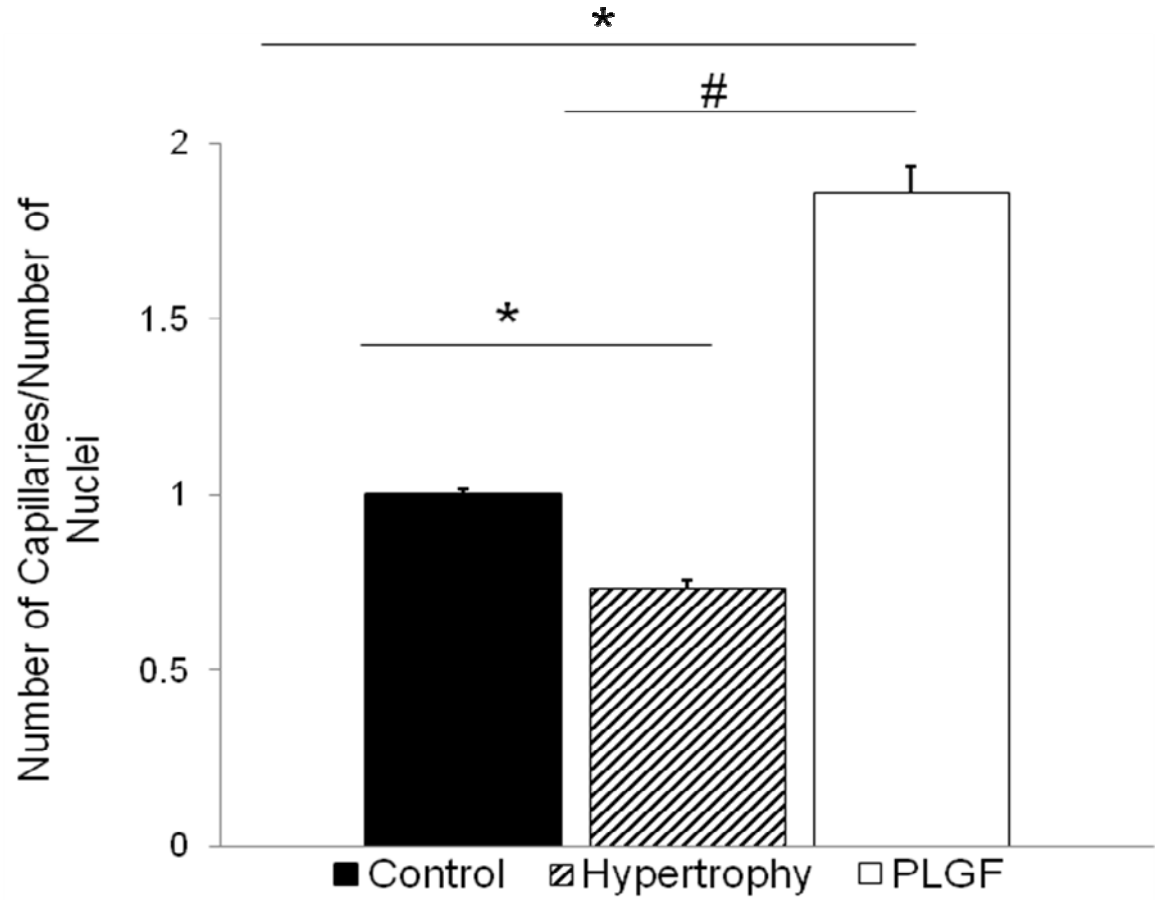

Figure 31. Capillary density of control, hypertrophied and PlGF treated myocardium. Capillary density is expressed per total number of nuclei. Blocking of sVEGFR-1 by PlGF resulted in capillary growth through release of VEGF. *p<0.001 versus control, #p<0.001 versus PlGF

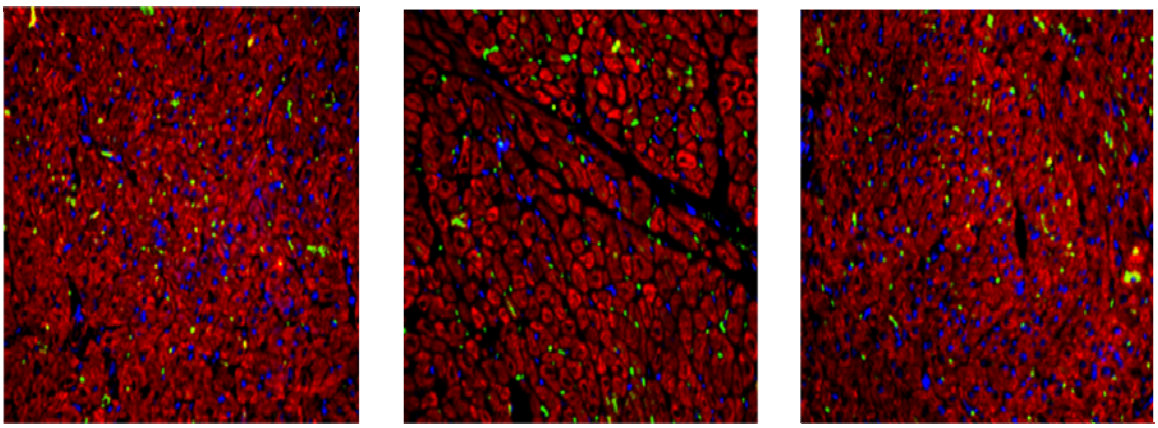

Control Hypertrophy Hypertrophy + PlGF

Figure 32. Representative immunohistochemistry sections are shown with capillaries stained with CD31 in green, cardiomyocytes with desmin in red and nuclei with DAPI in blue. Blocking of sVEGFR-1 by PlGF resulted in capillary growth through release of VEGF

c) Free, Unbound VEGF

Free, soluble VEGF protein levels were measured by ELISA in tissue lysates obtained from hypertrophied, PlGF treated and control hearts. Hypertrophied hearts showed decreased levels of free, soluble VEGF in comparison to control hearts (*$p<0.001$), indicative of a significantly higher amount of VEGF bound to sVEGFR-1. PlGF treated hypertrophied hearts showed significant increased levels of free, soluble VEGF compared to untreated hypertrophied hearts (*$p<0.001$). Data are expressed as mean±SEM.

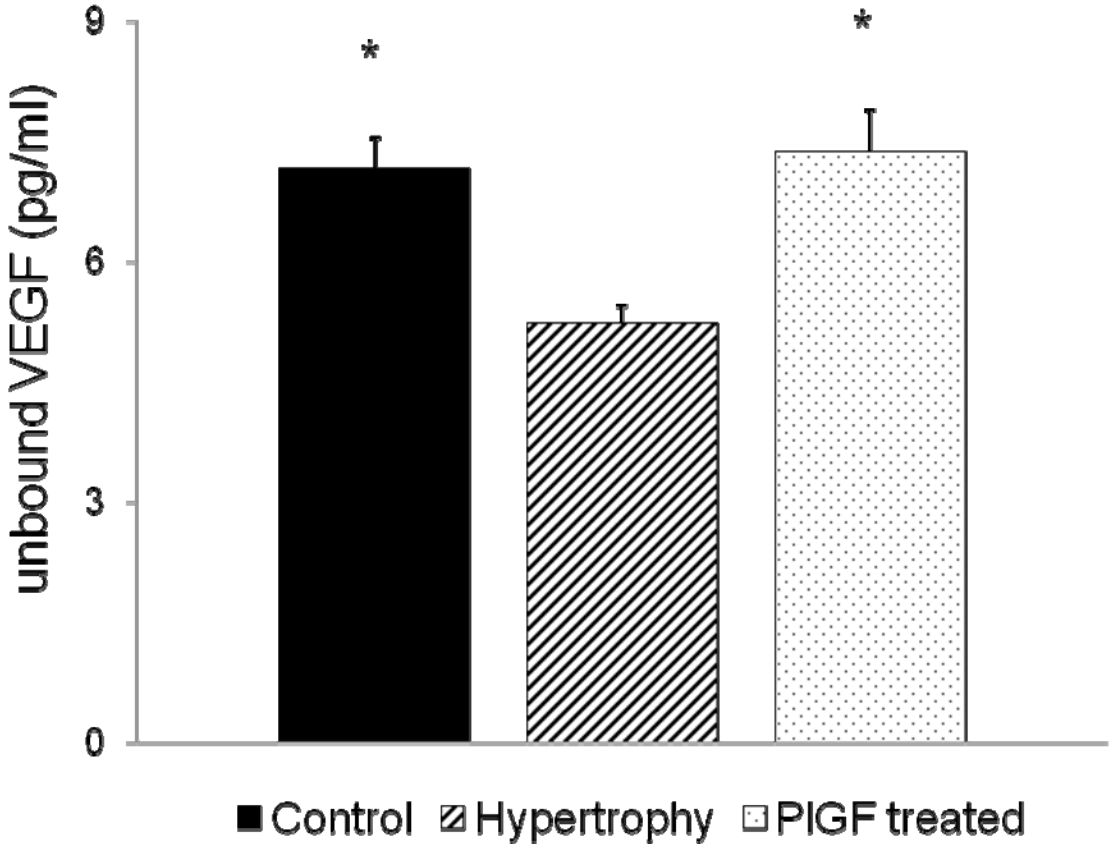

Figure 33. IHC staining with desmin (cardiac muscle, red), DAPI (nuclei, blue) and CD31 (capillaries, green) for control, hypertrophied and PlGF-treated tissue

d) mRNA Expression Levels- VEGF Isoforms

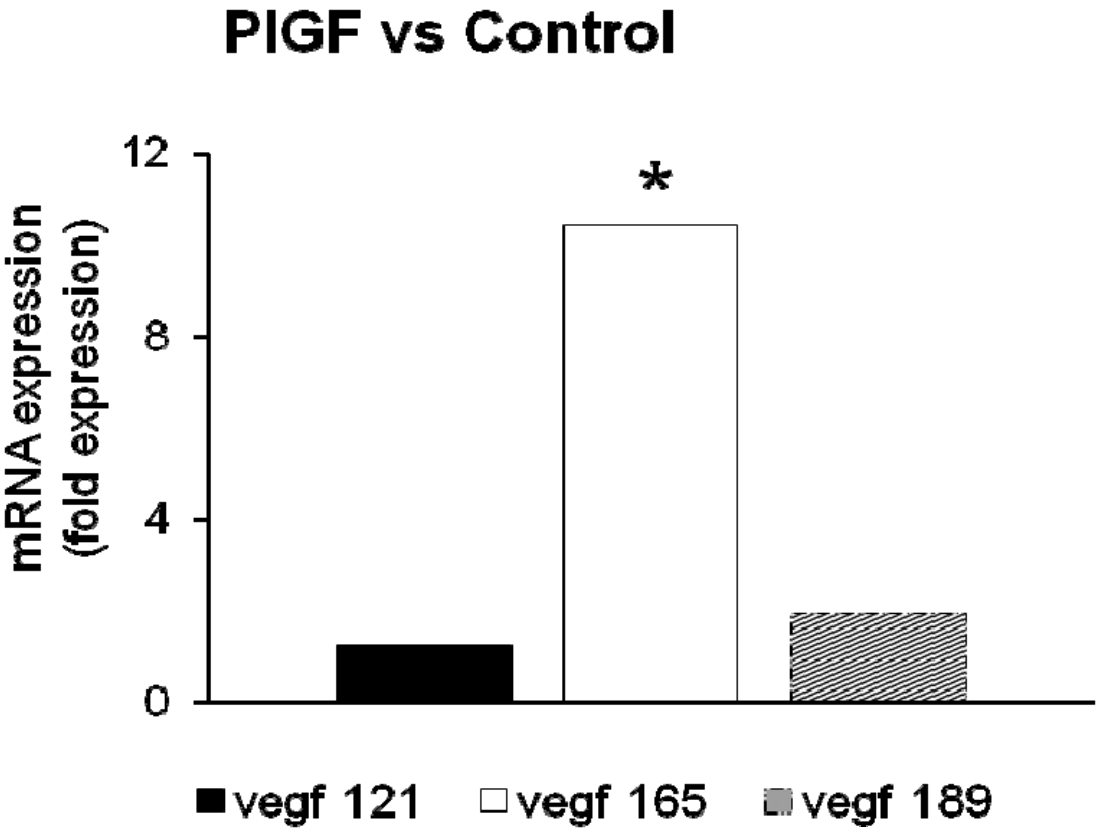
PlGF vs Control
mRNA expression (fold expression)
12
8
4
0
*
vegf 121
vegf 165
vegf 189

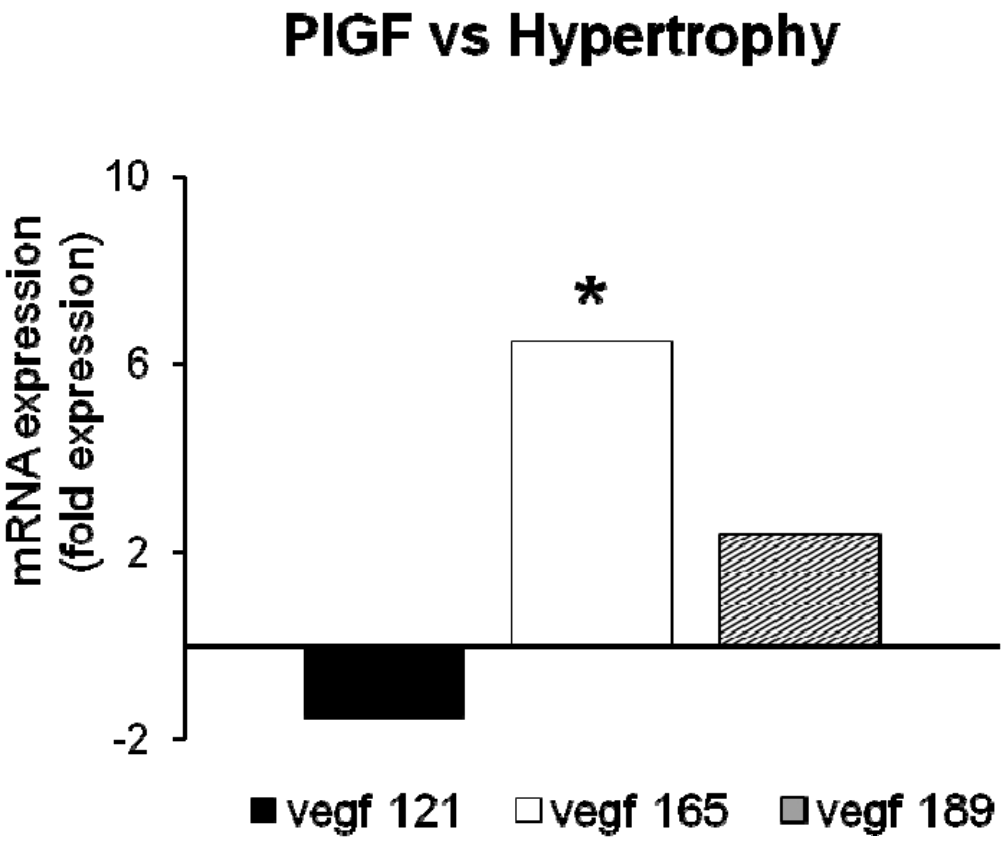

Figure 34. VEGF Isoform mRNA expression levels in PlGF versus hypertrophy and versus control hearts

Relative expression of mRNA of VEGF Isoforms VEGF121, VEGF165 and VEGF189 between control and PlGF treated and hypertrophied and PlGF treated hearts were shown in Figure 34.

VEGF165 was significantly up-regulated in PlGF treated animals (10 fold up-regulated vs Controls and 7 fold up-regulated versus hypertrophied myocardium; *$p<0.001$).

e) mRNA Expression Levels – total VEGF and VEGF Receptors

mRNA expression levels were obtained for total VEGF, the angiogenesis stimulating receptor VEGFR-2, VEGFR-1 and sVEGFR-1.

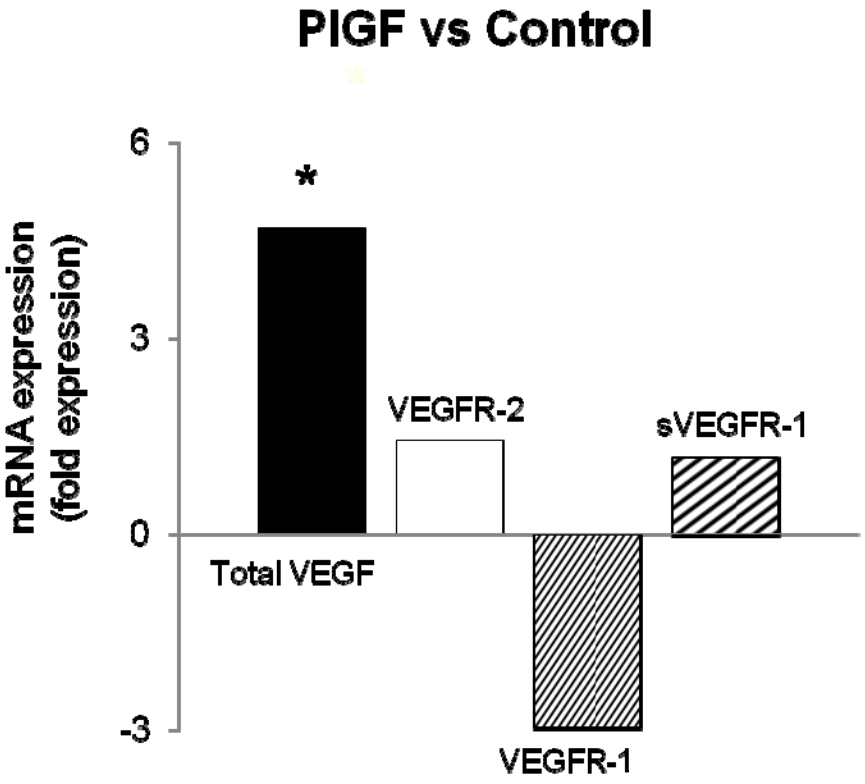

Figure 35. mRNA expression levels between PlGF treated hypertrophied and control hearts

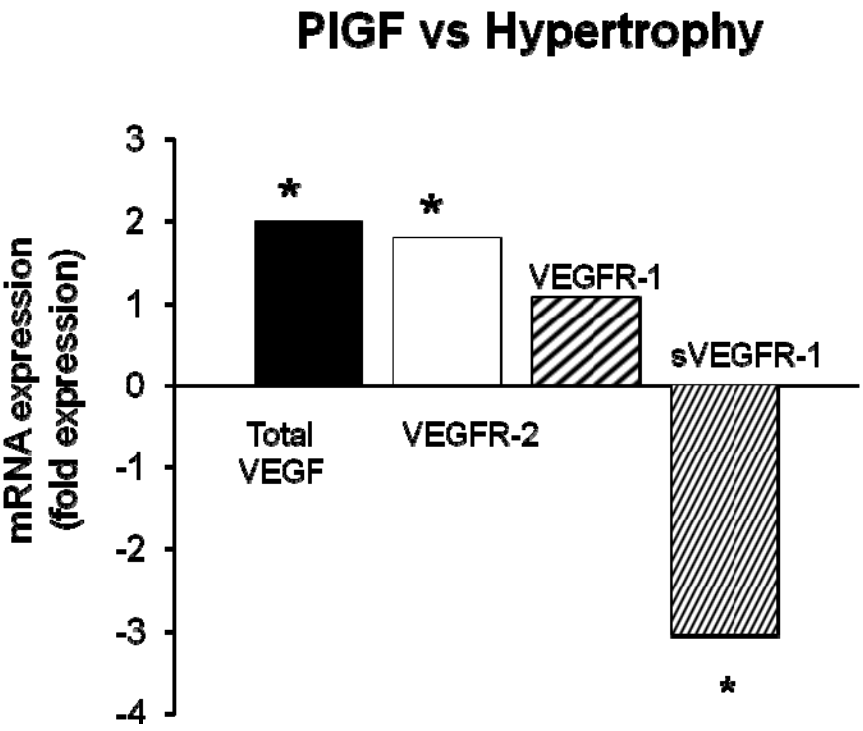

Figure 36. mRNA expression levels between PlGF treated hypertrophied and non-treated hypertrophied hearts

8. The glucose transport molecules GLUT1 and GLUT4 in pressure-overload myocardium

Specific primers were designed for qRT-PCR. Primer pairs for GLUT1 and GLUT4 are depicted below:

GLUT4 – Product Size: 66

AGCAGCTCTCAGGCATCAAT

CTACCCCTGCTGTCTCGAAG

GLUT1 – Product Size: 174

GCCCTGGATGTCCTATCTGA

CCCACAATGAAATTCGAGGT

GLUT1 mRNA expression level is significantly down-regulated in LV hypertrophy at six weeks of age (ventricular decompensation) when compared to age-matched control hearts (52.9% of control ± 9.1, p=0.0048).

In addition, mRNA expression of the insulin-dependent trans-membrane glucose facilitative transport molecule GLUT4 is significantly down-regulated in LV

hypertrophy at six weeks of age compared to age-matched controls (42.3% of control ± 15.2, p=0.0081).

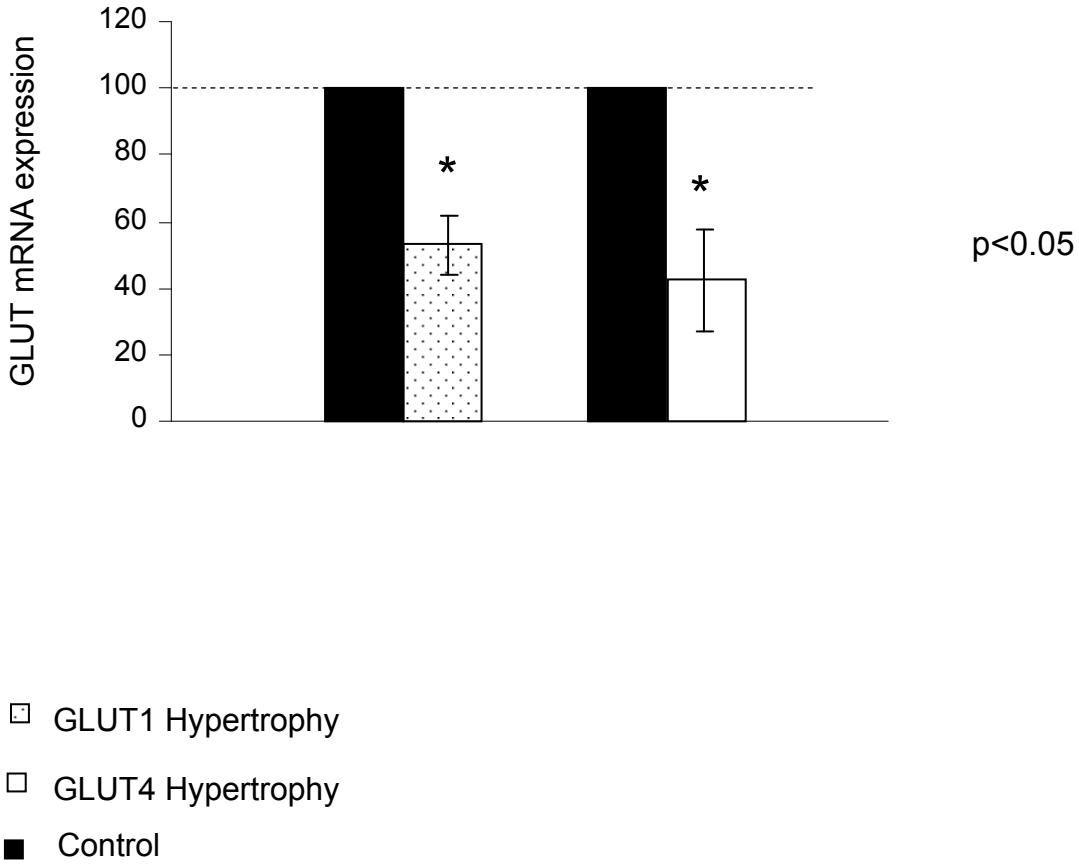

Figure 37. GLUT1 and GLUT4 mRNA expression level % of control

Discussion

DISCUSSION

The most important finding of this study is that VEGFR-1 and its soluble splice variant, sVEGFR-1, were significantly up-regulated in hypertrophied left ventricular myocardium at the onset of failure whereas the angiogenesis inducing receptor, VEGFR-2, was unchanged.

At the same time, total VEGF as well as all individual isoforms (VEGF121, VEGF165 and VEGF189) remained unchanged in pressure-overload hypertrophied myocardium and much of VEGF was bound to sVEGFR-1. We observed significantly lower levels of free, unbound VEGF in hypertrophied hearts, another indicative of VEGF sequestration by sVEGFR-1.

Blocking of the soluble VEGFR-1 with placental growth factor increased myocardial levels of free VEGF resulting in increased capillary growth. Thus, we concluded that increased levels of sVEGFR-1 sequester VEGF and thereby restrict the amount available for VEGFR-2 to induce angiogenesis in pressure-overload hypertrophied myocardium at the onset of failure.

Hypertrophy from pressure-overload is one of the most important sequelae of congenital and acquired heart defects and is a well known risk factors for cardiac surgery.

The progression of hypertrophy from compensated to decompensated, with ventricular dilation and contractile function and decreased tolerance to ischemia is a very important factor for long term survival from cardiac surgery.

In response to pressure-overload, changes and alterations occur in cardiomyocytes which are well described (Jalil 1988, Chapman 1990, Weber 1989). Cardiac hypertrophy leads to changes in the extracellular matrix (increased collagen deposition and alterations in the type and density). The coronary circulation is also altered in cardiac pressure-overload hypertrophy with a decrease in capillary density which is seen as hypertrophy progresses (Rakusan, 1976). The combined effect of myocyte hypertrophy and increased collagen deposition between myocytes and around capillaries results in an increase in diffusion distance with a potential for limiting delivery of oxygen and substrates for oxidative phosphorylation. This occurs particularly during states of high demand.

Decreased capillary density and coronary reserve play an important role in adaptation to increased work load.

Recognition of the potential role that decreased capillary density may play a part in the pathopysiology of pressure-overload hypertrophy will lead us to investigate new treatments and mechanism for the management of patients with this defect.

Development of better treatment strategies will further help us better understand the appropriate timing of surgical and/or non-surgical interventions which will eventually have a significant impact on decreasing the risk which is posed by myocardial hypertrophy.

Angiogenesis is a process, which is tightly regulated by various factors such as angiogenesis-stimulating (VEGF, Fibroblast Growth Factor) and endogenous angiogenesis-inhibitors (sVEGFR-1, angiostatin, endostatin). Further known angiogenesis growth factors are angiogenin, angiopoietin-1, granulocyte colony-stimulating factor, hepatocyte growth factor, leptin, placental growth factor, transforming growth factor alpha and beta and interleukin 8.

Known angiogenesis inhibitors are angiostatin, endostatin, heparinases, interleukin 12, metalloproteinase inhibitors, plasminogen activator inhibitor, retinoids, vasculostatin, vasostatin, prolactin 16kD, human chorionic gonadotropin and cartilage-derived inhibitor.

Fibroblast growth factors and angiopoietins and their receptors also play an important role not only in vessel formation but post-natal extension of the capillary network. Post-natal capillary growth occurs in response to hypoxia or to local effects of pro-inflammatory cytokines that induce activation and expression of the transcription factor (hypoxia inducible factor) responsible for a coordinated cellular response (Ferrara 1999, Klagsbrun, 1996, Oettegen, 2001). Endothelial cells are normally quiescent, but, however, in response to hypoxia, inflammation or locally produced growth factors, they undergo a change in morphology. This change includes the golgi apparatus, mitochondria and the endoplasmic reticulum. Transforming growth factor beta is a secreted growth factor which is released from cells undergoing apoptosis. This growth factor also contributes to

vessel formation by cooperatively inducing VEGF expression with hypoxia inducible factor (Shih 2001).

The process of angiogenesis leads to the formation of new blood vessels by sprouting from pre-existing microvasculature, and is essential for normal mammalian development. The process of angiogenesis occurs in a particular series of events. Injured tissues produce an angiogenic growth factor which is going to be released into the tissue. This growth factor binds to specific angiogenic receptors which are located on endothelial cells (EC) of nearby blood vessels. New molecules, enzymes are produced and signals are sent from the surface of the cell into the nucleus. Enzymes are able to form tiny holes in the basement membrane which surrounds the blood vessels. Adhesion molecules, called integrins, are specialized molecules which help the sprouting process. Matrix metalloproteinases are additional enzymes which are produced to dissolve tissue. The tissue around the vessel and the extracellular matrix is remodeled by these enzymes. Endothelial cells roll up to form a new blood vessel tube. Various vessel tubes connect with each other and form mature blood vessels. These newly formed blood vessels are further stabilized by surrounding cells.

One of the most important inducers of angiogenesis in the heart is VEGF. All major cell types in cardiac tissue including cardiac myocytes, fibroblasts, and endothelial cells, have been shown to produce VEGF.

The VEGF gene is located on the short arm of chromosome six (6p21.3) and is composed of eight exons and seven introns (Vincenti et al. 1996). Houck et al.

described the coding region of at about 14kb (Houck et al. 1991). Alternative splicing can generate different isoforms whereof $VEGF_{121}$, $VEGF_{165}$ and $VEGF_{189}$ have been found in the heart [23]. $VEGF_{121}$ and $VEGF_{165}$ are the most abundant and potent isoforms with $VEGF_{165}$ having the highest receptor affinity (Bacic, 1995).

VEGF induces the proliferation and movement of endothelial cells, remodeling of the extracellular matrix and the formation of capillary tubules. The $VEGF_{165}$ isoform is only active to induce angiogenesis as the freely soluble protein. A significant amount of $VEGF_{165}$ remains bound to the cell surface and the extracellular matrix and is inactive (Friehs, 2006). $VEGF_{165}$ lacks residues of exon six and $VEGF_{121}$ lacks residues of exon six and seven.

In contrast, $VEGF_{189}$ is almost completely sequestered in the extracellular matrix and has an insertion of 24 amino acids (Houck, 1991). Bioactive VEGF is generated by proteolytic cleavage (Park, 1993). Therefore VEGF protein becomes available to endothelial cells by two different mechanisms: as a freely soluble protein or following protease activation by release from extracellular membrane bound stores. VEGF exerts its cellular effects by binding to two high-affinity transmembrane tyrosine kinase receptors: VEGFR-1 and VEGFR-2 (Folkman 1995, 1992 and Jebreel, 2007). VEGFR-2 is the main receptor involved in VEGF-stimulated angiogenesis (Shibuya, 1990, Ferrara, 1999). However, most normal tissues do not express measurable levels of VEGF or its receptors (Dvorak, 1995 and Brown 1995).

During normal cardiac growth between childhood and young adulthood (physiologic hypertrophy), coronary microvascular growth parallels the degree of cardiomyocyte growth.

In pathologic hypertrophy, this tight relationship appears to be lost. As cardiomyocytes enlarge with hypertrophy, a mismatch develops between the number of capillaries and cardiomyocytes per unit area, suggesting that the volume of tissue supplied by one capillary increases. Increased pressure loading on the ventricle produces a sustained abnormal increase in myocardial wall stress, which leads to progressive ventricular remodeling.

The stress imposed on the cardiomyoyctes is a major stimulator for VEGF production and release (Seetharam, 1995). One would therefore expect increased production and release of VEGF and/or specific isoforms. As we have previously reported hypertrophying myocardium suffers from early onset of cardiomyocyte loss, which also potentially restricts the amount of VEGF released from the remaining hypertrophied cardiomyocytes (Friehs, 2006). It is therefore reasonable to conclude that mRNA levels of neither total VEGF nor any of the isoforms are up-regulated in the left ventricular hypertrophied myocardium because of insufficient production of the VEGF isoforms by the remaining hypertrophied cardiomyocytes.

At the same time, protein levels of VEGF were also unchanged which indicates that also matrix bound, thus stored VEGF, had been cleaved and released for binding to VEGF receptors and / or storage has not been adequately restored.

Another important finding of this research work was that mRNA expression levels of GLUT1 were significantly down-regulated in LV hypertrophy at six weeks of age (ventricular decompensation) when compared to age-matched control hearts. Glucose is an important source of energy for the heart. Glucose utilization and transport by cardiomyocytes is critical for normal cardiac function.

However, fatty acid oxidation is the major metabolic source of acetyl CoA for the tricarboxylic acid cycle (TCA cycle) in the normal working heart. Although glucose is not the predominant substrate in the normal heart, there are many situations in which it assumes greater importance such as increased workload and pressure-overload hypertrophy and ischemia.

Glucose is transported into cardiomyocytes by members of the family of facilitate glucose transporters (GLUTs). The most abundant facilitate glucose transporter in the myocardium is GLUT4.

The plasma membrane is impermeable to polar molecules such as glucose. The cellular uptake of glucose across the plasma membrane is mediated through glucose transporters, which reside in and span the plasma membrane. In addition, they are rate limiting of glucose entry in the cell. Trans-sarcolemmal glucose transport in cardiomyocytes is mediated by GLUT1 and GLUT4, which are expressed in high levels in the cardiac tissue.

Basal glucose transport is mediated primarily by GLUT1, which is constitutively present in sarcolemma but not in transverse tubules. GLUT4, which is the insulin-dependent trans-membrane glucose facilitative transport molecule, plays an

important role in insulin–dependent cardiac glucose metabolism. Under basal conditions, only a small amount of GLUT4 is located in the sarcolemma. GLUT4 is primarily localized in small tubulo-vesicular elements adjacent to the sarcolemma and transverse tubules, and in the trans-Golgi system. The translocation of glucose transporters, in particular GLUT4, to the sarcolemma and T-tubules is mainly regulated by insulin, exercise and ischemia.

As hypertrophy progresses, the metabolic state of the myocardium becomes more anaerobic which is indicated by an increased level of lactate dehydrogenase, particularly in subendocardial layers. Changes in calcium regulation, energy production and substrate metabolism occur at varying states during the progression from compensated hypertrophy to ventricular dilation and failure. All of theses systems have been shown to be altered in late stages and failing ventricles. Contractile protein isoform shifts and increased dependence on glucose metabolism appears to occure early on (Bishop 1970, Chevalier 1989). During the late period and in conjunction with failure, downregulation of the sarcoplasmic reticulum and the expression of glucose transporter are evident (Qi 1997). Decreased glucose uptake in response to insulin is an early marker of the transition from compensated to uncompensated pressure-overload hypertrophy (Takeuchi 1995, 1998).

In addition, mRNA expression of the insulin-dependent trans-membrane glucose facilitative transport molecule GLUT4 is significantly down-regulated in LV hypertrophy at six weeks of age compared to age-matched controls.

Fong et al. have shown that VEGFR-1 null mutant mice die at the embryonic stage (in utero) due to an overgrowth and disorganization of blood vessels and not due to poor vascularization (Fong et al, 1995), which indicates that VEGFR-1 is essential for the organization of embryonic vasculature but not for endothelial cell differentiation (Fong, 1995).

Events mediated through VEGFR-1 are mainly responsible for early stages of VEGF-induced angiogenesis, such as modulation of cell motility and adhesion of endothelial cells, whereas VEGFR-2 is more important in regulating endothelial cell proliferation (Seko, 1999).

The affinity of VEGFR-1 for VEGF is very high, with a Kd of about 2-10 pM, which is at least one order of magnitude higher than that of VEGFR-2 (De Vries, 1992). On the other hand, the tyrosine kinase activity of VEGFR-1 is relatively weak, and VEGF does not stimulate the proliferation of cells over-expressing VEGFR-1 (Seetharam, 1995 and Waltenberger, 1994).

Since VEGFR-1 and VEGFR-2 can form heterodimers, VEGFR-1 may participate in the regulation of the proliferative response of endothelium to VEGF (Shweiki, 1993).

This suggests VEGFR-1 to be both a negative regulator by sequestering (trapping) VEGF via its ligand-binding domain, and on the other hand, a positive regulator by its decoy function attracting VEGF or due to its mild tyrosine kinase signaling activity. VEGFR-1 is known to be a 180-kDa transmembrane protein

that is composed of seven extracellular immunoglobulin-like (Ig-like) domains, which include the binding site for VEGF in the second Ig-like domain, a single transmembrane domain and an intracellular tyrosine kinase region (Otrock, 2007, Waltenberger, 1994).

Another important feature of VEGFR-1 is that the gene encodes not only the mRNA for a full-length receptor but also a short mRNA for a soluble form of the VEGFR-1 Kenprotein which carries only the extracellular domain (Kendall, 2006 and Maynard, 2003) and has a unique 31 amino-acid C-terminus (Kendall 2006 an Waltenberger, 2003).

It was first reported in patients with pre-eclampsia who showed abnormally high levels of sVEGFR-1 associated with inadequate vascularization of the placenta (Maynard, 2003).

The soluble form of VEGFR-1 is likely to be a negative regulator of VEGF availability because it forms heterodimers with membrane-bound VEGFR-1 and VEGFR-2 thus acts as a receptor blocker of both VEGFR-1 and VEGFR-2 (Kendall, 2006) and also because it sequesters VEGF, limiting the amount of free, soluble VEGF for induction of angiogenesis.

Various research laboratories have shown that VEGFR-2 is the main mediator of VEGF-induced angiogenesis. Releasing VEGF by blocking sVEGFR-1 may displace VEGF from VEGFR-1 and sVEGFR-1, which makes it available for binding to VEGFR-2, a concept known as ligand shifting (Park, 1993).

Other growth factors are able to bind to VEGF Receptors, besides VEGF. Placental growth factor (PlGF) is a disulfide-linked dimeric protein which belongs to the same family as VEGF (Houck, 2002 and Kendall, 2006).

Placental growth factor (PlGF) is a disulfide-linked dimeric protein which belongs to the same gene family as VEGF (Kendall, 2006). Both receptors have distinct binding characteristics: VEGF exerts its biologic activities by interacting with both VEGF Receptors, VEGFR-1 and VEGFR-2, while PlGF interacts only with VEGFR-1/sVEGFR-1 but not with VEGFR-2 which potentially competes with VEGF for binding to VEGFR-1/sVEGFR-1.

VEGF is known to be an inducer of vascular permeability and angiogenesis in vivo. Endothelial cells in culture respond to VEGF with increased cell survival, proliferation and migration (Matsumoto, 2001). PlGF is angiogenic, chemotactic for endothelial cells (Clauss, 1996) and adult PlGF-null mutant mice demonstrate reduced angiogenesis and vascular leakage (Carmeliet, 2001).

As mentioned before, PlGF binds only to VEGFR-1/sVEGFR-1 but not to the angiogenesis inducing receptor VEGFR-2. Thereby, it may displace VEGF from VEGFR-1 to VEGFR-2 (Park 1994).

Our data are in support of the notion that PLGF's competitive binding to sVEGFR-1 releases VEGF trapped by this receptor. Up-regulation of VEGF by either exogenous application as we have previously shown or endogenously by releasing VEGF from sVEGFR-1 results in capillary growth (Friehs, 2003, 1999,

2006). It remains to be determined whether endogenous production of VEGF in the hearts treated with PlGF also plays a role.

In our model of pressure-overload hypertrophy, we found that both the full-length VEGFR-1 and its alternatively spliced soluble variant, sVEGFR-1, were significantly up-regulated.

Like VEGFR-1, sVEGFR-1 also has a 10-fold higher affinity to VEGF than VEGFR-2 and it binds all VEGF isoforms in the heart (Maynard, 2005, Kendall, 2006). The role of the full-length VEGFR-1 in modulation of angiogenesis in hypertrophied myocardium, however, remains to be determined.

Our results indicate that sVEGFR-1 was trapping VEGF, which restricted the amount of free, soluble VEGF for interaction with VEGFR-2 to induce angiogenesis. Lack of up-regulation of VEGF and at the same time trapping of VEGF by the angiogenesis inhibitor sVEGFR-1 resulted in inhibition of capillary growth in hypertrophied myocardium.

Strategies aimed at up-regulating VEGF or binding the soluble VEGFR-1 (with placental growth factor or certain antibodies) may be useful in maintaining capillary density and preventing heart failure.

REFERENCES

1. **Arnett DK, de las Fuentes L, Broeckel U.** Genes for left ventricular hypertrophy. *Curr Hypertens Rep. 2004; 6(1): 36-41. Review.*

2. **Bacic M, Edwards NA, Merrill MJ.** Differential expression of vascular endothelial growth factor (vascular permeability factor) forms in rat tissues. *Growth Factors* 1995; 12 (1):11-15.

3. **Bishop SP, Altshuld RA.** Increased glycolytic metabolism in cardiac hypetrophy and congestive heart failure. *Am J Physiol* 1970; 218: 153-159.

4. **Brown LF, Detmar M, Claffey K, Nagy JA, Feng D, Dvorak AM, Dvorak HF.** Vascular permeability factor/vascular endothelial growth factor: a multifunctional angiogenic cytokine. *EXS* 1995; 79:233-269.

5. **Chapman D, Weber KT, Eghbali M.** Regulation of fibrillar collagen types I and III and basement membrane type IV collagen gene ezxpression in pressure-overload rat myocardium. *Circ Res* 1990; 67(4):787-94.

6. **Chevalier B, Callens F, Charlemagne D, et al.** Signal and adaptational changes in gene expression during cardiac overload. *J Mol Cell Cardiol* 1989; 21:71-77.

7. **Colan SD.** Non-invasive serial evaluation of myocardial mechanics in pressure overload hypertrophy of rabbit myocardium. *Herz* 2003; 28(1):52-62.

8. **Dvorak HF.** Vascular permeability factor/vascular endothelial growth factor: a critical cytokine in tumor angiogenesis and a potential target for diagnosis and therapy. *J ClinOncol* 2002; 20(21):4368-80.

9. **De Vries C, Escobedo JA, Ueno H, Houck K, Ferrara N, Williams LT.** The fms-like tyrosine kinase, a receptor for vascular endothelial growth factor. *Science* 1992; 225:989-991.

10. **Dvorak HF, Brown LF, Detmar M, Dvorak AM.** Vascular permeability factor/vascular endothelial growth factor, microvascular hyperpermeability, and angiogenesis. *Am J Pathol* 1995; 146:1029-1039.

11. **Dvorak HF.** Angiogenesis: update 2005. J *Thromb Haemost. 2005; 3(8):1835-42. Review*.

12. **Ferrara N, Gerber HG, LeCouter J.** The biology of VEGF and its receptors. *Nat Med.* 2003; 9(6):669-76.

13. **Ferrara N.** Role of vascular endothelial growth factor in the regulation of angiogenesis. *Kidney Int* 1999; 56(3):794-814.

14. **Ferrara N, Henzel WH.** Pituitary follicular cells secrete a novel heparin-binding growth factor specific for vascular endothelial cells. *Biochem Biophys Res Commun. 1989; 161(2):851-8.*

15. **Folkman J, Haudenschild C.** Angiogenesis in vitro. *Nature. 1980; 288(5791): 551-6.*

16. **Folkman J.** Seminars in Medicine of the Beth Israel Hospital, Boston. Clinical applications of research on angiogenesis*. N Engl J Med* 1995;333(26):1757-63.

17. **Folkman J, Shing Y.** Angiogenesis. *J Biol Chem. 1992; 267(16):10931-4. Review.*

18. **Folkman J, Shing Y.** Control of angiogenesis by heparin and other sulfated polysaccharides. *Adv Exp Med Biol* 1992; 313:355-64.

19. **Fong GH, Rossant J, Gertsenstein M, Breitman ML.** Role of the Flt-1 receptor tyrosine kinase in regulating the assembly of vascular endothelium. *Nature* 1995; 376(6535):66-70

20. **Friehs I, del Nido PJ.** Increased susceptibility of hypertrophied hearts to ischemic injury. *Ann ThoracSurg* 2003; 75(2):S678-84.

21. **Friehs I, Moran AM, Stamm C, Colan SD, Takeuchi K, Cao-Danh H, Rader CM, McGowan FX, del Nido PJ.** Impaired glucose transporter activity in pressure-overload hypertrophy is an early indicator of progression to failure. *Circulation* 1999;100(19 Suppl):II187-93.

22. **Friehs I, Margossian RE, Moran AM, Cao-Danh H, Moses MA, del Nido PJ.** Vascular endothelial growth factor delays onset of failure in pressure-overload hypertrophy through matrix metalloproteinase activation and angiogenesis. *Basic Res Cardiol*. 2006;101:204-213.

23. **Friehs I, Barillas R, Vasilyev NV, Roy N, McGowan FX, del Nido PJ.** Vascular endothelial growth factor (VEGF) prevents apoptosis and preserves contractile function in hypertrophied infant heart. *Circulation* 2006; 114 (Suppl I):I290-5.

24. **Friehs I, Moran AM, Stamm C, Choi YH, Cowan DB, McGowan FX, del Nido PJ.** Promoting angiogenesis protects severely hypertrophied hearts from ischemic injury. *Ann Thorac Surg* 2004; 77(6):2004-10.

25. **Houck KA, Leung DW, Rowland AM, Winer J, Ferrara N.** Dual regulation of vascular endothelial growth factor bioavailability by genetic and proteolytic mechanisms. *J Biol Chem* 2002;267(36): 26031-260367.

26. **Hong DL, Zhang YZ, Piacibello W, Agliettam M.** Vascular Endothelial Growth Factor and Its Receptor KDR/flk-1 Play Important Roles in Hematopoiesis. *Zhongguo Shi Yan Xue Ye XueZaZhi* 2002;9 (3):268-272.

27. **Fruttiger M, Calver AR, Richardson WD.** Platelet-derived growth factor is constitutively secreted from neuronal cell bodies but not from axons. *Curr Biol. 2000; 10 (20):1283-6.*

28. **Jebreel A, England J, Bedford K, Murphy J, Karsai L, Atkin S.** Vascular endothelial growth factor (VEGF), VEGF receptors expression and microvascular density in benign and malignant thyroid diseases. *Int J Exp Pathol*. 2007;88(4):271-7.

29. **Jalil JE, Doering CW, Janicki JS, Pick R, Clark WA, Abrahams C, Weber KT.** Structural vs. contractile protein remodeling and myocardial stiffness in hypertrophied rat left ventricle. *J Mol Cell Cardiol* 1988; 20(12):1179-87.

30. **Karamysheva AF.** Mechanisms of angiogenesis. *Biochemistry (Mosc). 2008; 73 (7): 751-62. Review.*

31. **Kendall RL, Wang G, Thomas KA.** Identification of a natural soluble form of the vascular endothelial growth factor receptor, FLT-1, and its heterodimerization with KDR. *Biochem Biophys Res Commun* 2006;226:324–8.

32. **Kendall, R.L. and Thomas, K.A.** Inhibition of vascular endothelial cell growth factor activity by an endogenously encoded soluble receptor. *Proc Natl Acad Sci U S A*. 1993; 90(22): 10705-9.

33. **Leung DW, Cachianes G, Kuang WJ, Goeddel DV, Ferrara** N. Vascular endothelial growth factor is a secreted angiogenic mitogen. *Science* 1989; 246(4935):1306-9.

34. **Maglione D, Guerriero V, Viglietto G, Ferraro MG, Aprelikova O, Apilalo K, Del Vecchio S, lei KJ, Chou JY, Persico MG.** Two alternative mRNAs coding for the angiogenic factor, placenta growth factor (PlGF), are transcribed from a single gene of chromosome 14. *Oncogene; 8(4):925-31.*

35. **Maglione D, Guerriero V, Viglietto G, Delli-Bovi P, Persico MG.** Isolation of a human placenta cDNA coding for a protine related to the vascular permeability factor. *Proc Natl Acad Sci USA* 1991. 88(20):9267-71.

36. **Maynard SE, Venkatesha S, Thadhani R, Karumanchi SA.** Soluble Fms-like tyrosine kinase 1 and endothelial dysfunction in the pathogenesis of preeclampsia. *Pediatr Res*. 2005;57(5 Pt 2): 1R-7R.

37. **Maynard SE, Min JY, Merchan J, Merchan J, Lim KH, Li J, Mondal S, Livermann TA, Morgan JP, Sellke FW, Stillman IE, Epstein FH, Sukhatme VP, Karumanchi SA.** Excess placental soluble fms-like tyrosine kinase 1 (sFlt1) may contribute to endothelial dysfunction, hypertension, and proteinuria in preeclampsia. *J. Clin. Invest.* 2003; 111, 649-658.

38. **Maxwell PH, Pugh CW, Ratcliffe PF**. The pVHL-HIF-1 system. A key mediator of oxygen homeostasis. *Adv Exp Med Biol 2001;502:365-76. Review.*

39. **Meyer RD, Mohammadi M, Rahimi N.** A single amino acid substitution in the activation loop defines the decoy characteristic of VEGFR-1/FLT-1. *J Biol Chem* 2006; 281(2):867-75.

40. **Meyer M, Clauss M, lepple-Wienhues A, Waltenberger J, Augustin HG, Ziche M, Lanz C, Buttner M, Rziha HJ, Dehio C.** A novel vascular endothelial growth factor encoded by Orf virus, VEGF-E, mediates angiogenesis via signaling through VEGFR-2 (KDR) but not VEGFR-1 (Flt-1) receptor tyrosine kinases. *EMBO J. 1999; 18(2):363-74.*

41. **Moran AM, Friehs I, Takeuchi K, Stamm C, Hammer PE, McGowan FX, del Nido PJ, Marti HH.** Vascular endothelial growth factor. *Adv Exp Med Biol. 2002;516:375-394.*

42. **Otrock ZK, Makarem JA, Shamseddine AI.** Vascular endothelial growth factor family of ligands and receptors: review. *Blood Cells Mol Dis* 2007, 38(3):258-68.

43. **Park JE, Keller GA, Ferrara N.** The vascular endothelial growth factor (VEGF) isoforms: differential deposition into the subepithelial extracellular matrix and bioactivity of ECM-bound VEGF. *Mol Biol Cell* 1993; 4:1317-1326.

44. **Persico MG, Vincenti V, DiPalma T**. Structure, expression and receptor-binding properties of placenta growth factor (pIGF). *Curr Top Microbiol Immunol. 1999; 237:31-40.*

45. **Qi M, Shanon TR, Euler DE, Bers DM, Samarel AM.** Downregulation of sarcoplasmic reticulum Ca2+ ATPase during progression of left ventricular hypertrophy. Am J Physiol 1997. 272, H2416-H2424.

46. **Pfaffl MW, Horgan GW, Dempfle L.** Relative expression software tool (REST©) for group-wise comparison and statistical analysis of relative expression results in real-time PCR. Nucleic Acids Res. 2002; 30(9):e36.

47. **Rakusan K, Flanagan MF, Geva T, Southern J, VanPraagh R.** Morphometry of human coronary capillaries during normal growth and the effect of age in left ventricular pressure-overload hypertrophy. *Circulation* 1992, 86:38-46.

48. **Ribatti D.** The discovery of the placental growth factor and its role in angiogenesis: a historical review. *Angiogenesis. 2008; 11(3):215-21.*

49. ***Rozen S and Skaletsky H.*** *Primer3 on the WWW for general users and for biologist programmers. Methods Mol Biol 2000, 132:365-86.*

50. **Senger DR, Connolly DT, Van de Water L, Feder J, Dvorak HF**. Purification and NH2-terminal amino acid sequence of guinea pig tumor-secreted vascular permeability factor. *Cancer Res. 1990;50(6):1774-8.*

51. **Senger DR, Perruzzi CA, Feder J, Dvorak HF.**A highly conserved vascular permeability factor secreted by a variety of human and rodent tumor cell lines. *Cancer Res. 1986, 46(11): 5629-32.*

52. **Seetharam L, Gotoh N, Maru Y, Neufeld Gm Yamaguchi S, Shibuya**. A unique signal transduction from FLT tyrosine kinase, a receptor for vascular endothelial growth factor VEGF. *Oncogene* 1995; 10, 135-147.

53. **Seko Y, Takahashi N, Shibuya M, Yazaki Y.** Pulsatile stretch stimulates vascular endothelial growth factor (VEGF) secretion by cultured rat cardiac myocytes. *Biochem Biophys Res Commun* 1999; 254(2):462-5.

54. **Shen BQ, Lee DY, Gerber HP, Keyt BA, Ferrara N, Zioncheck TF.** Homologous up-regulation of KDR/Flk-1 receptor expression by vascular endothelial growth factor in vitro. *J BiolChem* 1998; 273(45):29979-29985.

55. **Shibuya M, Yamaguchi S, Yamane A, Ikeda T, Tojo A, Matsushime H and Sato M.** Nucleotide sequence and expression of a novel human receptor-type tyrosine kinase gene (flt) closely related to the fms family. *Oncogene* 1990; 5: 519-524.

56. **Shinkaruk S, Bayle M, Lain G, Deleris G.** Vascular endothelial cell growth factor (VEGF), an emerging target for cancer chemotherapy. *Curr Med Chem Anticancer Agents* 2003; 3(2):95–117.

57. **Takeuchi K, Buenaventura P, Cao-Danh H, Glynn P, Simplacenau E, McGowen FX, del Nido PJ.** Improved protection of the hypertrophied left ventricle by histidine containing cardioplegia. *Circulation* 1995. 92:II395-399.

58. **Takeuchi K, McGowen FX, Glynn P, Moran AM, Radar CM, del Nido PJ.** Glucose transporter upregulation improves ischemic tolerance in hypertrophied failing heart. *Circ*. 1998; 98: II234-241.

59. **Tischer E, Mitchell R, Hartman T, Silva M, Gospodarowicz D, Fiddes JC, Abraham JA**. The human gene for vascular endothelial growth factor. Multiple protein forms are encoded through alternative exon splicing. *J Biol Chem. 1991;266(18):11948-54.*

60. **Tjwa M, Luttun A, Autiero M, Carmeliet P.** VEGF and PlGF: two pleiotropic growth factors with distinct roles in development and homeostasis. *Cell Tissue Res. 2003; 314(1):5-14. Review.*

61. **Vincenti V, Cassano C, Rocchi M, Persico G.**Assignment of the vascular endothelial growth factor gene to human chromosome 6p21.3. *Circulation. 1996; 96(8):1493-5.*

62. **Vuorela P, Hatva E, Lymboussaki A, Kaipainen A, joukov V, Persico MG, Alitalo K, Halmesmaki E.** Expression of vascular endothelial growth factor and placenta growth factor in human placenta*. Biol Reprod. 1997; 489-94.*

63. **Waltenberger J, Claesson-Welsh L, Siegbahn A, Shibuya M, Heldin CH.** Different signal transduction properties of KDR and Flt1, two receptors for Vascular Endothelial Growth Factor. *J. Biol. Chem* 1994; 269: 26988-26995.

64. **Weber KT.** Cardiac interstitium in health and disease: the fibrillar collagen network. *J Am Coll Cardiol* 1989; 13(7): 1637-52.

ABBREVIATIONS

% SF	-	Shortening fraction
Ang 1	-	Angiopoietin
EGF	-	Epidermal Growth Factor
ELISA	-	Enzyme linked immunoassay
ES	-	Endothelial cells
FGF	-	Fibroblast Growth Factor
Ig	-	Immunoglobulin
Kb	-	Kilobase
Kd (kDa)	-	Kilo Dalton
M/V ratio	-	Mass/Volume Ratio
NOS	-	Nitrous Oxide Systems
PDGF	-	Platelet-derived Growth Factor
PlGF	-	Placental Growth Factor
qRT PCR	-	Revere Transcription Polymerase Chain Reaction
sVEGFR-1	-	Soluble Vascular Endothelial Growth Factor Receptor 1
TGF-beta	-	Transforming Growth Factor
VEGF	-	Vascular Endothelial Growth Factor
VEGFR-1	-	Vascular Endothelial Growth Factor Receptor 1
VEGFR-2	-	Vascular Endothelial Growth Factor Receptor 2
WB	-	Westernblot

FIGURES AND TABLES

FIGURES

TABLES